TUM School of Engineering and Design

Characterization of Sheet Molding Compound (SMC) materials for automotive applications.

Carmen Cholvi Mifsud

Scientific Thesis for Acquiring the Bachelor of Science Degree at the Department of Mechanical Engineering of the Technical University of Munich.

Supervisor	Univ.-Prof. Dr.-Ing. Klaus Drechsler Chair of Carbon Composites
Advisor	Anna Julia Imbsweiler, M.Sc. Chair of Carbon Composites
External Advisor (if applicable)	Dipl.-Ing. Mia Extern Firma Muster GmbH
Author	Carmen Cholvi Mifsud Tübinger Straβe 3 80686 München Tel.: +34 683 522 591 Matr.-Nr.: 03795137
Submission Date	22.07.2024 in Garching near Munich

Technical University of Munich
TUM School of Engineering and Design
Chair of Carbon Composites
Boltzmannstraße 15
D-85748 Garching near Munich

Tel.: +49 (0) 89 / 289 – 15092
Fax: +49 (0) 89 / 289 – 15097
Email: info.lcc@ed.tum.de
Web: www.asg.ed.tum.de

PROJECT ASSIGNMENT

Lehrstuhl für Carbon Composites
Fakultät für Luftfahrt, Raumfahrt und Geodäsie
Technische Universität München

Bachelor's Thesis, Term project, Master's Thesis

Characterization of Sheet Molding Compound (SMC) materials for automotive applications.

Sheet Molding Compound (SMC) with carbon fibers is a type of composites very attractive for the automotive industry. The material is made of carbon fibers cut into chips (typical length of 25 mm) and randomly dispersed in a resin system. SMC can be processed into complex components in a short period of time by compression molding. This allows engineers to readily use the existing parts design knowhow and achieve lighter components with higher strength. Automakers have already adopted SMC for automotive doors, inner panels and structural components. One of the greatest advantages of SMC is that fibers remaining from other processes can be chopped to the necessary length and recycled into a new SMC material.

In a current project we aim at building new parts with SMC obtained from the scrap of the winding process. Due to logistical difficulties, the material obtained from winding by our project partner in Argentina has to be replicated here. In order to evaluate the transferability of the results obtained from tests performed here, tests have to be performed to characterize the material and compare the results to the results obtained for the Argentinian material. To this purpose, suitable tests such as tensile testing and squeeze flow tests have to be identified, performed and the results shall be directly compared.

Figure 1: Rear door frame made of SMC[Toyota]

Figure 2: Lightweight wheel rims[Blackwave]

Research Focus of the Thesis

- Literature research on the SMC material and material testing for SMC
- Selection and design of experiments for the necessary tests
- Measurement and evaluation of relevant properties
- Assessment of the comparison of the Argentinian and our material
- Documentation

Requirements

- Structured and precise way of working
- Experience with characterization methods is an advantage, but not a requirement

Starting date: Now

For more details please contact:
Anna Julia Imbsweiler, M.Sc. Room 5504.1.404, Tel. +49 89 / 289 – 15085, anna.julia.imbsweiler@tum.de

DECLARATION OF HONOR

I hereby declare on my honor that I have prepared this thesis independently and without the use of other than the indicated resources; the thoughts taken directly or indirectly from outside sources (including electronic sources) are identified as such without exception.

The work has not been submitted in the same or similar form to any other examination authority.

München, 22.07.2024

CARMEN| CHOLVI| MIFSUD

Firmado digitalmente por CARMEN|CHOLVI| MIFSUD
Fecha: 2024.07.22 17:45:57 +02'00'

City, Date Signature

ACKNOWLEDGMENT

I would like to express my gratitude to my supervisor Anna Julia Imbsweiler for her continuous support, guidance, and encouragement throughout the project. I would also like to sincerely thank my industry advisor, Gabriel Eduardo Rojas Valenzuela, for his support in the testing performance.

I would like to additionally thank Reiner Rauch, for his help in the workshop. Finally, I would like to acknowledge my family, especially my parents and my sister for their unconditional support through this research. This thesis would have not been possible without their contributions.

ABSTRACT

This thesis focuses on developing a suitable material for a hydrofoil surfboard by evaluating BMC and SMC materials, characterized by long fiber reinforcement. The primary aim is to compare the mechanical characteristics of six different material combinations, specifically evaluating the potential of BMC material against the industrially available SMC material.

The variability between BMC and SMC materials is assessed through tensile and flexural tests. In terms of Young's modulus, the different composite materials demonstrate better flexural properties than tensile characteristics, with higher results in the flexural test. However, the materials support higher tensile loads than flexural loads, resulting in higher UTS values in the tensile test compared to the flexural test.

After comparing the obtained results with the currently available data, it can be affirmed that the plates from this thesis exhibit better mechanical properties than the previously tested plates.

CONTENTS

NOMENCLATURE

Symbol	Unit	Description
A_0	$[mm^2]$	Initial cross-sectional area
b	$[mm]$	Width
E	$[MPa]$	Young's modulus
E^{chord}	$[GPa]$	Tensile chord modulus of elasticity
F	$[N]$	Compressive strength
h	$[mm]$	Thickness
k	$[N/m]$	Stiffness
L	$[mm]$	Support span length
L_f	$[mm]$	Final length
L_g	$[mm]$	Extensometer gage length
L_0	$[mm]$	Initial length
P	$[N]$	Maximum load
ε	$[mm/mm]$	Tensile strain
ε_f	$[mm/mm]$	Flexural strain
ε_{UTS}	$[mm/mm]$	Ultimate tensile strain
σ	$[MPa]$	Tensile stress
σ_f	$[MPa]$	Flexural stress

Symbol	Unit	Description
$\boldsymbol{\sigma_{UTS}}$	$[\boldsymbol{MPa}]$	Ultimate tensile strength
$\boldsymbol{\Delta L}$	$[\boldsymbol{mm}]$	Increase of length
$\boldsymbol{\Delta \varepsilon}$	$[-]$	Difference between two strain points
$\boldsymbol{\Delta \sigma}$	$[\boldsymbol{MPa}]$	Difference in applied tensile stress between two strain points

ABBREVIATIONS

Abbreviation	Description
BMC	Bulk Molding Compound
BVID	Barely Visible Impact Damage
CFRP	Carbon Fiber-Reinforced
CM	Compression Molding
CT	Compression Test
CVID	Clearly Visible Impact Damage
FRP	Fiber-Reinforced Polymeric
FT	Flexural Test
FW	Filament Winding
IR	Infrared
IT	Impact Test
MSFW	Multi-Stage Filament Winding
SMC	Sheet Molding Compound
SOM	Strength of Materials
SQT	Surface Quality Test
TT	Tensile Test
UTS	Ultimate Tensile Strength
UTM	Universal Testing Machine
WP	Winding Process

1 Status quo

Within the array of initiatives proposed by the European Commission for the automotive sector, two important aspects must be emphasized: the reduction of greenhouse gas emissions and the management of the end-of-life disposal of cars [1]. A desirable solution to reduce the environmental impact is the use of materials or components that can be reused as raw materials in a new process. Although getting back the raw materials from finished parts is very energy-intensive, the environmental impact is reduced by recovering part of the energy lost during manufacturing of the raw material [2]. Another important factor is that there is a need to reduce the waste of carbon composite fibers due to the accumulating production waste during typical manufacturing processes is estimated to be as high as 50%. Therefore, using fibers as raw material in new processes involves not only new opportunities for circularity but also a wide variability of quality requirements in lightweight applications [3]. Sheet Molding Compound (SMC) and Bulk Molding Compound (BMC) have the potential to help in this situation. SMC and BMC are long fiber-reinforced materials that can adopt complex shapes with reduced weight, retaining mechanical properties and dimensional accuracy over a very wide temperature range [4].

This project reduces the environmental impact by using carbon fibers, derived from the waste of the winding process (WP). The fibers are cut to the required length and mixed with the resin matrix to achieve new composite components with the best mechanical properties. By using carbon fibers, the weight of the components can also be reduced compared to other materials such as steel or aluminum. This weight reduction leads to greater fuel efficiency and lower emissions. This material, which is produced by a compression molding (CM) process, is recognized by high volume production as it is more economical than other methods and the production is characterized by its high variability.

To obtain the final product, SMC and BMC composites are formed or cured by compression processes. They are considered sophisticated processes, as they are known not only for processing complex components within short cycle times but also for achieving lightweight components with suitable strength, considering that are lower than for endless fibers. However, this promising technology also has its challenges.

1.1 Motivation

This work aims not only to compare the mechanical characteristics and properties of composite laminates but also to look for a way to improve the composite material. The characteristics and properties of both materials, SMC and BMC are examined to subsequently evaluate and compare the differences and similarities between them to achieve the best material for our application. The selected material will be applied to a wing of the support in a hydrofoil surfboard. The assessment of the results is based on the characterization of six plates through flexural and tensile tests. Even if a product with appropriate processing is expected, several defects can occur during the testing process or the manufacturing of the material.

This research involves conducting tests, so it provides the chance to increase knowledge by learning new methods and the advances that can be achieved. In addition, not only more experience is gained with the testing machines and the behavior of the composites, but also is experimentally proved that the results do not always match the theory, but that does not mean that they do not represent progress.

Finally, it is important to emphasize that this project is part of an improvement of the carbon composite material. For this reason, this work is more than just a research project, it is a contribution to the advancement of future materials for automotive applications.

1.2 Objectives

Within this thesis, two types of processes, SMC and BMC, are evaluated considering their respective material composition. Their characteristics and properties are examined to subsequently evaluate the differences and similarities between them. Tensile and flexural tests are performed on samples produced using SMC and BMC in which carbon fibers are randomly dispersed in a resin system. During the test procedure, any defects that occur are analyzed. At the end of the test procedure, the relevant properties are measured, evaluated, and compared with the theoretical values. Once we have analyzed the results, they are compared to see how the mechanical properties are affected by small changes to the samples.

The main objective is to compare the results between six laminates. Two of them were produced from the WP waste processed with the BMC by the Argentinian partner. Two

more laminates are produced using the SMC, although this process does not benefit from the WP waste, the laminates are produced as a commercially available SMC process. In the commercial SMC, the fibers are inserted between two layers of a resin paste by randomly chopping fibers onto a plastic sheet film on which a paste of a resin and hardener mixture has been manipulated. Immediately, another film on which the paste mixture has been applied is placed on top, creating a sandwich structure of resin mixture and chopped carbon fibers. This structure is compacted by several rollers to wet the fibers and mix the constituents. The two last panels are produced by using BMC repeating the composition of the Argentinian's laminates. According to the best mechanical properties, and tensile and flexural behaviors, the most suitable laminate will be chosen, and specific adjustments to the test procedures will be made.

The automotive sector is very aware of its impact on the environment, so facts such as the reduction of waste must be taken into account. This fact not only reduces the waste of carbon fibers but also recovers the energy lost during the manufacturing of the raw material.

Lastly, the tests characterize the differences between the materials. Therefore, depending on the properties of each plate, conclusions are drawn about the suitability of the respective material for a specific application.

1.3 Structure

Following the Status Quo, the State of the Art is introduced, which evaluates the main methodologies: WP, SMC, and BMC, the CM technique, and the main tests to evaluate future defects in Chapter 2. Additionally, Chapter 3 describes the preparation of the plate and the specimens, and it defines the procedure of mechanical testing. After realizing the testing procedure, the results are analyzed and discussed in Chapter 4. Finally, a summary and outlook are conducted in Chapter 5. Figure 1-1 shows the review of the thesis structure.

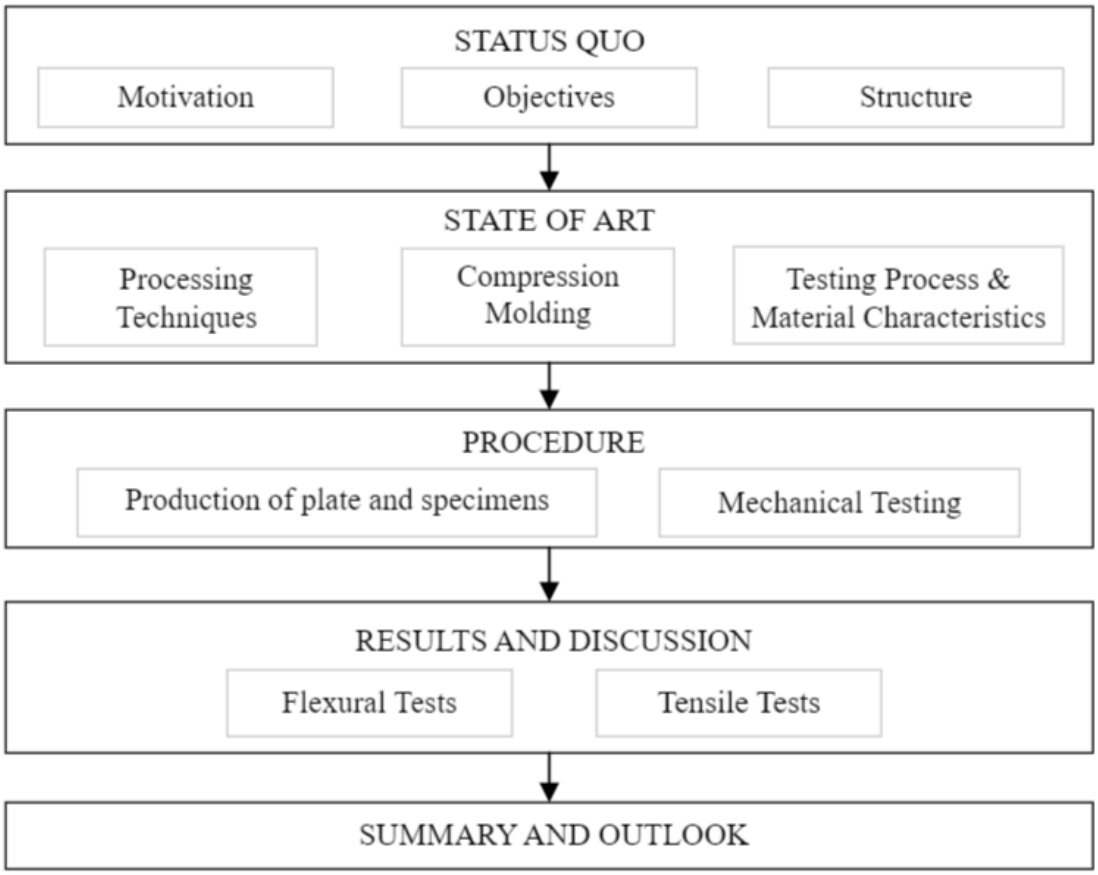

Figure 1-1: Review of the thesis structure

Various laminates are being investigated as part of this work. Part of the research studied in this project is also carried out by KOHLENIA S.A.'s Argentinian partners. They have produced two laminates with the BMC using carbon fibers from the waste of the WP. To find out how comparable both processes, BMC and SMC, are, five panels are analyzed. To assess the results of the different materials, including the evaluation of the corresponding mechanical properties and possible defects, it is necessary to carry out appropriate tests such as tensile and flexural tests.

2 State of the Art

Reducing greenhouse gas emissions, managing the end-of-life disposal of cars, and decreasing the waste of carbon composite fibers are relevant facts to be considered. To solve this situation, this research makes use of materials that can be reused as raw materials in a new process. Although the manufacturing of the raw material is energy-intensive, the environmental impact is reduced by recovering the lost energy during the already-stated manufacturing. In addition, by using the composite fibers from the scrap of WP the amount of waste of carbon fibers is decreased.

On the one hand, SMC and BMC processes have the potential to help in this situation, because complex shapes with reduced weight can be achieved by using fiber-reinforced materials. On the other hand, these methods are considered a technological challenge because of ensuring mechanical properties, dimensional accuracy, and variability in quality. To improve the composite material, the mechanical characteristics and properties of SMC and BMC laminates are compared. To evaluate and compare the respective results, TT and FT are performed, and the defects and discrepancies between theoretical and practical results are discussed. Finally, the material with the most suitable characteristic for the hydrofoil surfboard wind is selected.

This research is relevant to the State of the art for three reasons. It reduces the environmental impact, advances knowledge in the use of SMC and BMC, by offering insights into the behavior of composites under different conditions, and ensures that the new material selection reaches the requirements for the application.

This chapter consists of three sections. Section 2.1 describes the processing techniques investigated in this thesis. This section is divided into three subsections in which the three most important manufacturing processes are described: WP, SMC, and BMC, and their main characteristics. Section 2.2 examines the main process for processing the final product of the SMC and BMC processes, known as compression molding. Finally, section 2.3 lists the different tests for an adequate and complete evaluation.

2.1 Processing Techniques

To achieve a suitable material, there are three main processing techniques to be considered: WP, SMC, and BMC. The first technique to be described is the WP, as it is the starting point to get the fibers to produce the BMC laminates. Forthwith, SMC and BMC processes are defined.

2.1.1 Winding Process

The WP, also known as filament winding (FW), is considered the preferred method in the composites industry. This is because this technique is considered the most cost-effective, as it takes advantage of using fiber-reinforced polymers (FRP) to produce pressure-retained structures [5].

There are two different winding processes: wet winding and prepreg winding. In this study, wet winding was chosen because it has many advantages compared to prepreg winding, such as savings in winding time and material cost [6]. This mechanism can be used to produce structures with cylindrical and tubular shapes, such as high-pressure containers, rocket engine cases, launch tubes, fishing rods, and golf club shafts [7].

As for the materials, this research focuses on the fibers and the resin. On the one hand, this technique has three types of fibers that are wound on the rotating mandrel: long fibers (rovings), pre-impregnated fibers (prepregs), or wide fiber bundles (tapes). In general, there are three types of fibers, namely glass, carbon, and aramid fibers. The matrix resin, on the other hand, consists of a thermosetting resin, usually unsaturated polyester resins, or epoxy resins [8]. Before describing the influence of the material on the mechanisms, the process should be defined.

In the past, FW machines had little technical equipment in the early years. This process has been used since 1940, initially for applications in rocket technology by Richard E. Young, who was the first to present it to the US government. In addition, all processes were carried out manually for the first 40 years. The method consisted of loading mandrels, mixing the resin, and adding it to the resin bath. Immediately, the fibers were tied into the mandrel to begin the WP, and if necessary, the changes between the different

types of fibers in the FW were also made. Finally, the rovings were cut off and the wet-wound mandrels were placed in the oven.

This method is currently automated. This technology includes a complete system in which the mandrels are loaded with robots or manual devices. The resin mixing systems are mounted in the resin bath using a level meter and the required amount of premixed resin is dispensed into the resin bath. In addition, a fully automatic binding tool for wet or prepreg roving has been invented for the mandrel with a cutting device. They are re-tied onto the next mandrel and the wound parts are loaded into a curing unit [9]. The process is described below (see Figure 2-1) [10].

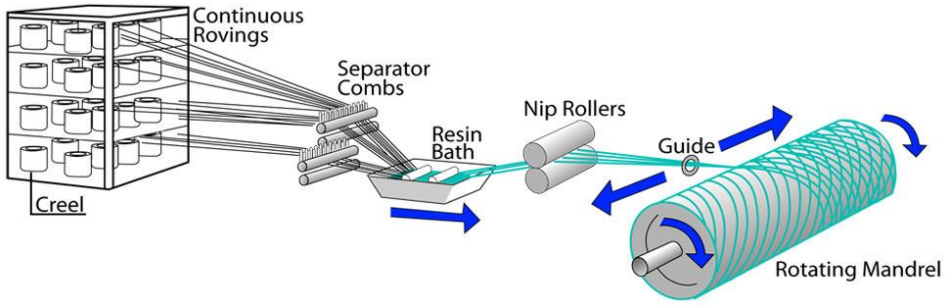

Figure 2-1: Filament winding process

The respective process consists of a fiber thread that is wetted with the required amount of resin and then winds evenly and regularly around a rotating mandrel through the corresponding resin path. After resin impregnation, the composite material is curved by heating it at a certain temperature in an oven or autoclave, where it is exposed to infrared (IR) radiation, and the mandrel lifts off.

An important point to emphasize is that the fibers traditionally rotated around only one axis. Nowadays, the fibers are lifted by moving a guide around pivot points or by rotating a mandrel around multiple axes [11]. Although this method has its advantages, as it is an automated and robotic process, it also has its disadvantages due to the geometrical limitations of the available tools. This method cannot be wound on negatively curved (concave) surfaces [12]. In case concave surfaces need to be produced, there is another method of WP, Multi-Stage Filament Winding (MSFW) [8].

This method currently uses patterns, that specify the number of bands to be placed in the mandrel. Important mechanical properties such as the mandrel geometry, the fiber angle, and the winding pattern influence the laminate thickness and the thickness distribution of

the layer. The layers are wound into the mandrels and a corresponding angle is assumed depending on the winding pattern [8]. There are two types of patterns in this technique: helical winding and biaxial winding. The first choice consists in defining a specific angle and it is characterized by its simplicity. The second choice is based on selecting two winding angles (0º and 90º) and is characterized by giving the structure a particular design and characteristics [13]. The wrapping angles of the helical winding can vary within the following limits, which range between low angles “in longitudinal direction” which means that the layer is oriented in the same direction as the mandrel, and high angles “as hoops” which approach 90º and are almost perpendicular to the mandrel axis.

Having described the procedure, it is important to take a closer look at the winding materials. This project will focus on the two main elements of the material: the fibers and the resin.

The carbon fibers will be used as pre-impregnated fibers, also called prepregs, which will form the basis to produce new components by the BMC process. The length of the fibers of the released material varies between 50 and 100 mm and it has a fiber volume ratio of 60%. To improve the flow properties of the mixture, the fibers are shortened to 10 mm, 14 times the critical fiber length. This length improves workability and ensures optimum load transfer. The fresh resin is then added.

The resin is an important component of the composite material. The composite material depends on this element, as the mechanical properties and material behavior can vary depending on the processing time and the parameters used. Epoxy resins, which are used in this project, are characterized among the polyesters and vinyl esters by their toughness and higher reactivity, which gives them the ability to bond well with fillers and reinforcing materials.

To take advantage of this method, there are several techniques for processing this material as a raw material. SMC and BMC have been classified as useful methods for producing new components [14]. The main goal of the project is to evaluate the differences and similarities between the BMC process and the SMC technique, considering that BMC used the scrap of the WP and SMC employed the characteristic materials of the technique. This research is also carried out by the Argentinian partner, and it aims to develop a new SMC material from recycled fibers, proving its processability and automatic manufacture [15].

2.1.2 Sheet Molding Compound (SMC)

SMC is known to be one of the most successful technologies for fiber-reinforced composites in the automotive sector [16]. This technique was introduced in the 1960s, and it introduced a new technology based on the employment of recycled fibers to be used in structural parts. This method is known for enabling lightweight components with high strength in short cycle times. First, the most important components are described. Then, the manufacturing process in the SMC line is explained.

The composition is based on four main components: thermosetting resins, fibers, and fillers, but this project focuses on the fibers and the resin. This method does not use prepregs made from the waste of the WP but uses the materials that are usually used in a standard performance. In our application, the carbon fibers are randomly oriented. They are chopped to 10 mm in length and the resin is added to produce the planned mixture. A typical SMC contains 30-50 wt% of fiber. This mixture is processed in a compression molding (CM) process to produce the respective laminates.

The resin is considered an indispensable component of the composite material, not only because it helps to bind the fibers, but also because it influences the mechanical properties of the CFRP, for example, the strength or the interlaminar fracture toughness. Resins are divided into two groups: thermosetting and thermoplastic resins. Thermosetting resins have a lower molecular weight and can be irreversibly crosslinked with carbon fibers [13]. Since an important goal of the automotive industry is weight reduction, this project will be targeted at this group. There are several distinctions between the multiple methodologies.

It is important to explain the differences between resin treatment in the WP and SMC process. Firstly, the gelation of the mixture can take up to 6 hours in WP, but in SMC, the maturation takes at least a week before molding. In both procedures, the temperature is 25 ºC. Moreover, the mold filling speed is a significant factor in SMC, which is controlled by the closing speed of the press, whereby a slower speed during the last few millimeters can prevent some molding defects. Another important factor is the temperature. Although WP cures at 100 ºC, SMC can be cured up to 145 ºC.

Now that we have analyzed the main materials that will make up the future composite panel, it is going to take a closer look at the manufacturing procedure. The SMC process is based on two main phases: compounding and maturation (see Figure 2-2) [17].

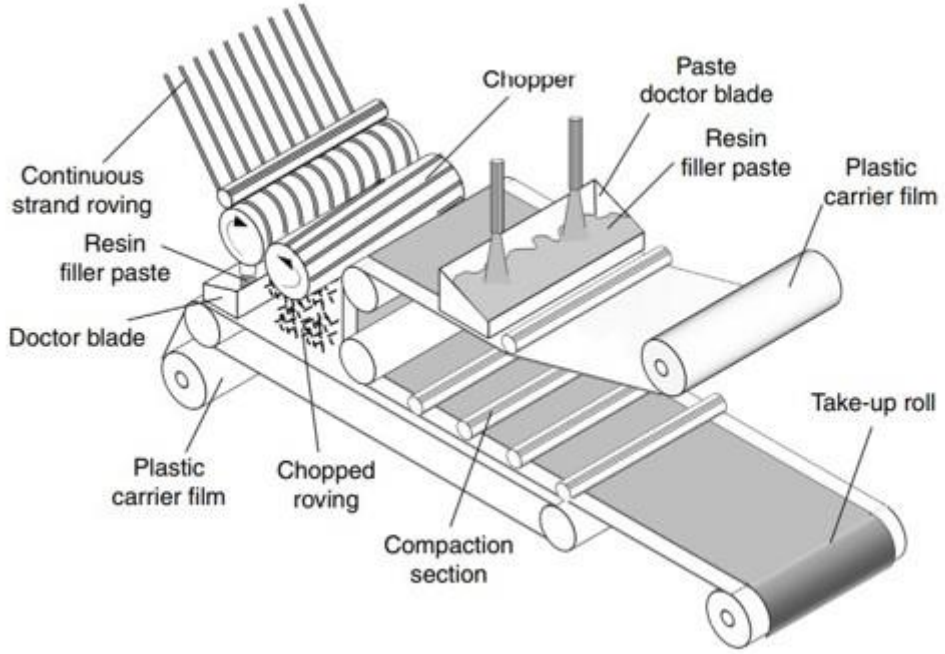

Figure 2-2: SMC manufacturing process

In the first phase, the fibers are inserted between two layers of a resin paste by randomly chopping fibers onto a plastic sheet film on which a paste of a resin and hardener mixture has been manipulated. Immediately, another film on which the paste mixture has been applied is placed on top, creating a sandwich structure of resin mixture and chopped carbon fibers. This structure is compacted by several rollers to wet the fibers and mix the constituents. In the maturing stage, the resin is cured to mold viscosity and ensure easy handling and rolled up for shipping [17]. To process the finished mixture into a sandwich structure, the CM process can be used.

2.1.3 Bulk Molding Compound (BMC)

A significant amount of waste is generated during the wet WP, which accounts for around 10% of the production [15]. To solve this problem, the BMC technique is presented. This process benefits from a scrap of the wet WP by using the prepregs as raw material for the production of new BMC parts.

This procedure is based on a combination of chopped carbon fibers, resin, and fillers. Although this technique is scant similar to the SMC process such as the resin formulation, it also has some differences (see Table 2-1: Properties of BMC and SMC processesTable 2-1) [17].

Table 2-1: Properties of BMC and SMC processes

Empty Cell	**BMC**	**SMC**
Glass fiber content (%)	10-25	25-35
Density (gcm^{-3})	1,8-2	1,5-1,7
Tensile strength (MPa)	28-55	82-138
Tensile modulus (GPa)	3,4-10.3	6,2-13,8
Flexural strength (MPa)	69-172	172-276
Flexural modulus (GPa)	5,5-8,3	6,9-8,3
Notched Izod impact energy (KJm^{-1})	0,15-0,55	0,55-1,1
Coefficient of thermal expansion ($10^{-6}{}^{o}C^{-1}$)	4,5-8,3	5,5-10

In general, the mechanical properties of BMC are lower than those of SMC. This process differs from SMC for two main reasons. On the one hand, the fiber length is shorter than that of SMC, since this process uses fibers with a length of 10-25 mm, while the SMC process contains fibers with a length of 25-35 mm. On the other hand, the content of reinforcing fibers such as glass fibers is 5-10% lower than in SMC. These differences have a relevant influence on the strength and tensile modulus [17].

There are three main materials to produce the BMC mixture: the prepregs from the waste of the WP, the epoxy resin, especially the EC 14, and the hardness, especially the W 282. The BMC production process is similar to the SMC process.

BMCs are produced by cutting the prepregs to the required length, in particular 10 mm. The mixture of the resin, hardener, and fibers is mixed until it is completely uniform. The paste is then crushed with a roller to obtain a square form. The fiber length influences the strength. If the goal is to achieve higher strength, long fibers must be used. If the main purpose is to obtain more complex structural parts, the length of the fibers must be shorter. Moreover, the stiffness can be improved by adding rids [18].

There are three types of procedures to produce the final product of BMC. These are the compression molding, which is currently used, the transfer molding, and the injection

molding. In our application, the CM process is used, which is described in the next chapter.

2.2 Compression Molding

This procedure is an important manufacturing technique to reduce the waste of carbon fiber composites and contributes to sustainable development in lightweight applications. This method is used in two molding processes: BMC and SMC. However, despite our application having mainly been tested and carried out on BMC parts, this process has been applied to both techniques, SMC and BMC laminates.

In this project, a laminate manufactured in Argentina was reproduced. It has the following composition:

- Fibers mass: 329,5 g
- Resin mass: 214,7 g
- Hardener mass: 56,8 g

The CM procedure is based on the following steps. The mixture obtained from the BMC process is placed in a mold, heated, and compacted under high pressure. As a rule, this process is carried out through a careful program. Depending on the procedure, this technique takes several minutes or hours, and the parameters are selected to reach certain properties. Various parameters such as the temperature, the pressure, or the waiting time until the press is lowered, influence the mechanical properties of the samples and the possible future defects. The methodology is illustrated and described below (see Figure 2-3) [17].

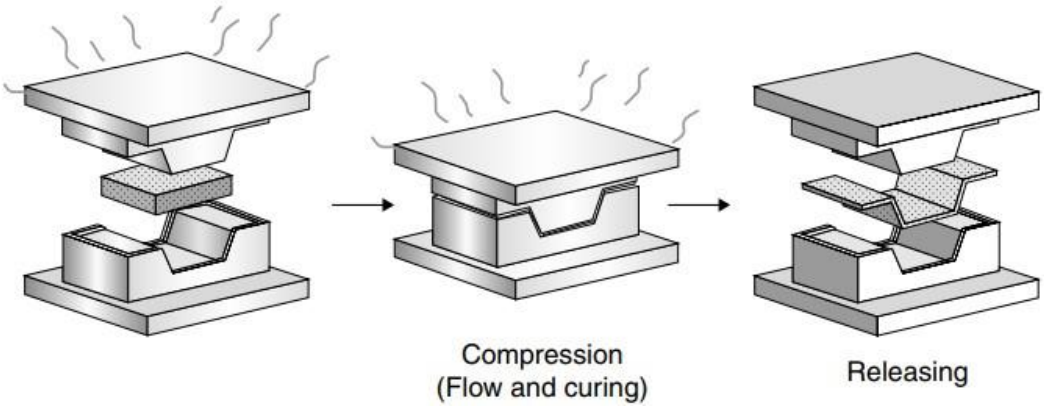

Figure 2-3: Compression molding process

In CM, the mixture is placed in the lower half of an adapted metal mold. This mold is compressed and expanded to cure the material. A similar method is used in the SMC process.

This process enables cost and weight savings through the production of a large series of composite parts in a short cycle time. The use of BMC from chopped fibers in compression molded parts allows for higher strength, lower weight, and higher performance with reduced tooling costs. In particular, CM reaches complex shapes that cannot be produced with continuous long fiber composites when using thermoset-based composites. An important point to consider is the tolerances, in mold construction, especially in the core and cavity halves. Although this method is considered a potential technology and procedure, various defects can occur. There are different types of defects, and depending on the size of the defect, it is recognized by the corresponding method. Furthermore, defects are also related to the atmosphere or the composition of the material, for example, the inclusion of air. Other possible causes are misalignment defects, in the resin matrix, and machine errors. In contrast to fibers and resin, the trapped air can be released again, whereas this is not possible with fibers and resin [18]. Air entrapment can occur during the manufacturing process. Incorrect alignment errors reduce relevant properties such as modulus or strength. Defects can also occur in the resin matrix, such as cavities, impurities, and resin-rich areas, which can be detected using atomic force microscopy or X-ray radiography. Defects related to machine faults such as drilling or cutting can be detected by visual and optical tests. All of these defects can appear in the form of delamination, cracks, and burrs [19].

2.3 Testing Process and Material Characteristics

To evaluate the possible defects that can occur during the manufacturing process and their influence on the mechanical properties, several tests must be performed. There are five interesting tests: tensile test (TT), compression test (CT), flexural test (FT), impact test (IT), and surface quality test (SQT). Before having a look at the tests in more detail, some of the reasons for their importance will be explained.

2.3.1 Tensile Test

This technique is a mechanical measurement in which a standardized specimen is subjected to an increasing tensile force until it fractures. To predict the material behavior properties such as the ultimate tensile strength (UTS), modulus of elasticity *E*, stress-strain curves, and stiffness are determined. The strength is considered a significant attribute for TT, and it measures the required amount of stress to appreciate the phenomenon of plastic deformation. This test also determines the maximum stress that a specimen can handle before becoming elongated (UTS).

Related to the machines, this technique can be performed through a Universal Testing Machine (UTM). A common standard specimen for sheet tensile testing is the *ASTM D3039* which has the characteristic dimensions of 25 mm in width and 250 mm in length [20]. The standardized dimensions coincide with the respective dimensions used in our application. There are two types of specimens: rectangular and tubular (see Figure 2-4) [21,22]. The test is realized with a rectangular specimen, which involves a few changes in the process.

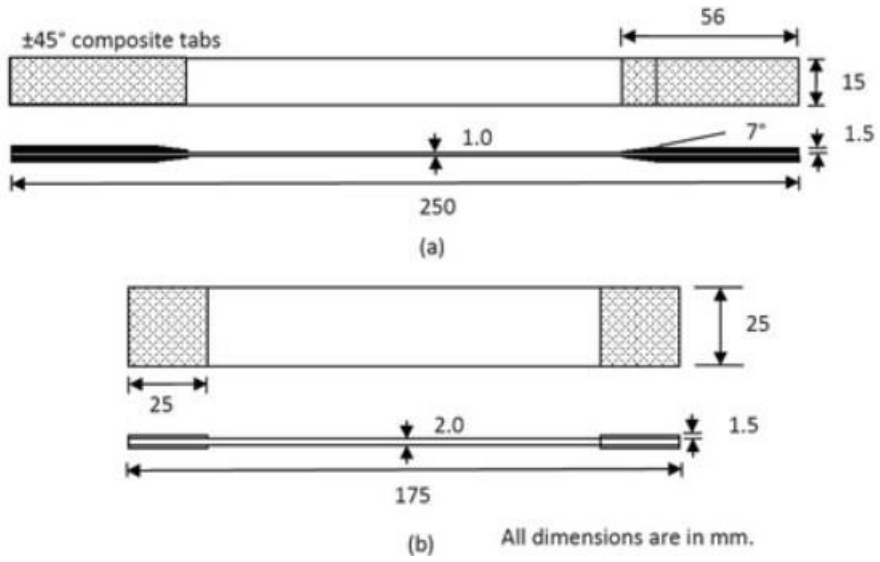

Figure 2-4: Rectangular specimens: a) ASTM D3039 for 0º, b) ASTM D3039 for 90º, and c) Tubular tensile specimen

The standard recommends the use of tabs with reinforcement at ± 45º. Moreover, end-tabs can also enable accurate alignment of the specimen in the test machine because they are positioned symmetrically and properly on the specimen. The tabs are pasted to the specimen firmly with adhesive and are used to protect the specimen material from being damaged by the grips. The TT is performed on coupons with 0º laminate for corresponding axial properties and coupons with 90º laminate for corresponding transverse properties.

The gage cross-sectional area experienced a reduction compared to the remainder of the specimen. The principal reason for this fact is that it has been applying an increasingly loaded tensile force between both ends of the specimen, hence, it has produced a deformation on the gage region. The corresponding measures are taken in this gage area. Another fact that we can esteem is the variation of the gage length. The fact that the gage cross-sectional area has been diminished, involves that the gage length has increased.

Once it has visually identified the evolution of the material after employing the load, it is relevant to emphasize the testing properties to assess the mechanical properties of the composite. Presently, this project will target stress-strain curves to transform magnitudes of force-elongation into engineering known as well as stress-strain data.

The stress-strain curve is an indispensable analysis of the material because it reveals some of the most important properties of the composite. If we consider an original specimen with any tensile force F applied, it can be defined by a cross-sectional area A_0 and an

initial length L_0. However, if we employ an increasing force between both ends, we can notice that the gage region experiments some changes that have been already mentioned such as the reduction of the gage cross-sectional area and the increase in length. Depending on the composition of the specimen, it will take longer or lower to reach the fracture.

The stress describes the relationship between the force applied in the initial cross-sectional area and the strain explains the relationship between the variation of the length regarding the initial length, and they are defined with the following formulations, respectively:

$$\sigma = \frac{F}{A_0} \quad \textbf{(2-1)}$$

$$\varepsilon = \frac{\Delta L}{A_0} \quad \textbf{(2-2)}$$

$$\Delta L = L_F - L_0 \quad \textbf{(2-3)}$$

where σ is the stress, ε is the strain, and L_F is the final length after having applied the force, and they are defined through the stress-strain curve. Equation 2-3 quantifies the variation of the length in the gage section. This characteristic curve can be divided into two zones. The first one is the elastic region. Its particularity resides in the ability of the material to recuperate the original shape when the stress is removed. The slope of this lineal section is defined by the formulas:

$$\mathrm{E} = \frac{\Delta\sigma}{\Delta\varepsilon} \quad \textbf{(2-4)}$$

where E is the Young's modulus, $\Delta\sigma$ is the difference in applied tensile stress between two strain points, and $\Delta\varepsilon$ is the difference between two strain points, nominally 0.002 [23].

Nevertheless, the second zone works at higher stresses, and its deformation is not recovered. Moreover, the stiffness is determined by the following formula:

$$k = \frac{EA}{L_g} \quad \textbf{(2-5)}$$

Where L_g is the extensometer gage length.

2.3.2 Compression Test

This technique has turned into a relevant method that determines the polymer matrix composite laminates behavior in the automotive sector. Regarding CT techniques, it is important to highlight three different methods of transmitting compression force: *Test Method D695* which is recognized by employing the load into the specimen by end loading, *Test Method D6641 / D6641M* which is popular by using a mixture of end loading procedure and the shear loading process, and *Test Method D5467M* which is famous by using a honeycomb core sandwich with thin skins to apply the burden (see Table 2-2) [24].

Table 2-2: Comparison of composite compression test methods

Test	Nominal Specimen	Unsupported gauge length	Critical Parameters	Comments
ASTM D5467 & D7249	24" X 1" bonded to a sandwich beam	0"	Specimen uniformity	Expensive specimen to fabricate and rarely used.
ASTM D3410 (IITRI)	5.5" X 1"	0.5"	Symmetry of Tabs	Large, heavy fixture
ASTM D695	3.13" X 0.5" dogbone	0"	End flatness	For woven materials only
SACMA SRM 1R-94	3.13" X 0.5" tabbed	0.188"	End flatness, fixture torque	Provides higher relative values
ASTM D6641	5.5" X 0.5" or 1"	0.5"	End flatness, fixture torque	Most common method, has unsupported length and is easier to use

It can be appreciated the different dimensions of the specimens used according to the respective standards, the unsupported gauge length, the critical parameters, and some advising notes about each method.

Our application is based on laminated polymer composite material, hence within this thesis, the standardized specimen ASTM D6641 is selected [25]. This characteristic standardization includes the dimensions of 140 mm in length and 12 mm in width. This

procedure establishes the compressive strength and stiffness of the sheets by employing a mixture of two compression methods: shear and end loading. The clamping force is applied to the center of the specimen which has any support on it (see Figure 2-5) [26].

Figure 2-5: Custom Test Fixture

This application takes advantage of the test fixture of 12 mm in gage length without any support in the center of the test specimen. The specimen is introduced into two platens of the test fixture and tightened with 8 screws by using a torque wrench to guarantee its fastening. This technique is carried out by a test fixture hitched in a universal testing machine where the specimen gets compressed until failure.

Within the testing method, several mechanical characteristics are studied such as compressive strength, and compressive modulus. The compressive strength is defined in the formula:

$$F = \frac{P}{A} = \frac{P}{h \cdot b} \qquad \textbf{(2-6)}$$

The compressive strength F is the result of the division of the maximum load that has been applied P to the specimen by its area A, equivalent to the product of the width b of the specimen and the thickness h [27]. The strain measurement is carried out with individual strain gauges employed in the center on both sides. The corresponding gauges produce signals that allow for assessment of the compressive strain. Moreover, it already exists another measurement procedure equivalent to the strain. In case the gauge length is free enough, which means being at least 12.7 mm implemented in the center of the

specimen, there is a form that improves the accessibility by taking advantage of the test fixture with a two-sided measuring clip-on extensometer [26].

2.3.3 Flexural Test

This method is one of the most important tests to characterize a CFRP. The FT consists of measuring the stiffness and strength properties of the material by employing the necessary force to bend it. This testing method makes use of the standard specimen ISO 14125 [28] . The length must be 20% longer than the support span. These tests can be carried out through three types of machines: the UTM, the four-point flexural fixture, and the three-point flexural fixture (see Figure 2-6) [29]. This study emphasizes the three-point flexural test.

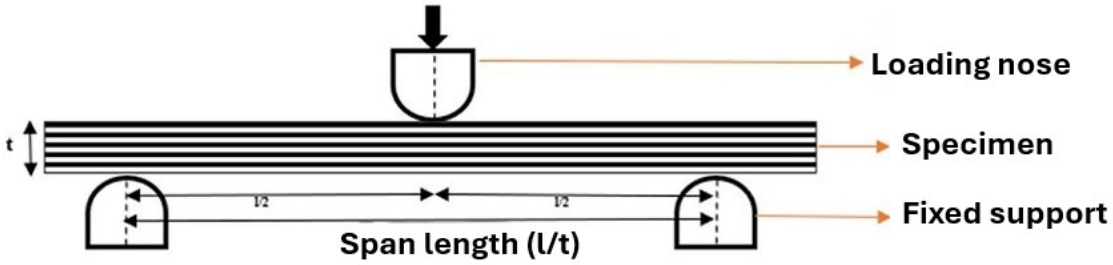

Figure 2-6: Three-point flexural test

The specimen is submitted to a three-point bending load, with two points placed on the ends of the specimen which supports the structure, while a moving load pin holds the last point positioned at the mid-span of the specimen. Several mechanical properties such as flexural strength, stress-strain curve, and flexural modulus of elasticity are determined by the following equations, respectively.

$$\sigma_f = \frac{3FL}{2bh^2} \quad \textbf{(2-7)}$$

$$\varepsilon_f = \frac{6sh}{L^2} \quad \textbf{(2-8)}$$

$$E_f = \frac{L^3}{4bh^3} \quad \textbf{(2-9)}$$

Where *L* is the support span length, *b* is the width, *h* is the thickness, and *s* is the deflection of the center of the specimen.

Flexural properties such as quality control, specification purpose, and the design of applications influence the material finish and its properties [16].

Thickness is a relevant property of this testing method since the dimensions of the specimens depend on their thickness. Table 2-3 shows the standard adapted dimensions.

Table 2-3: Standard dimensions of each group of specimens

Plate	Thickness (mm)	Width (mm)	Length (mm)	Span Length (mm)
K1	2,75	25	50	40
K2	2	25	50	40
T1	2,25	25	50	40
T2	3,25	10	65	52
L	4-4,25	10	80	64

This research is based on thickness variability, and it is proven through the Strength of Materials (SOM) formula which is defined as:

$$\sigma_f = \frac{1{,}5 \cdot P_{max} \cdot L}{b \cdot h^2} \quad \textbf{(2-10)}$$

Another essential property is the flexural stress-strain curve, which is based on a linear region, an abrupt drop in the flexural stress, and a plastic region. In the plastic region, it has noticed a considerable reduction of the experimental flexural modulus remains constant for a determinate range of flexural strain until the structural failure. The slope of the flexural stress-strain curve is used to calculate the flexural modulus while employing a small strain (0.001 to 0.003 mm/mm) [30]. The maximum strength can be written in the stress-strain curve. Additionally, the standardized value of the span-to-thickness ratio is 32:1.

2.3.4 Impact Test

Within the automotive industry, IT is considered a great technique to assess the behavior and properties of composite materials but also forms part of the quality control processes. Impact tests allow us to determine the material response under different impact conditions. Intending to evaluate the resulting force and displacement, this method makes use of an impact on a composite material from a particular distance, angle, and velocity. The performance takes place in a controlled environment such as measurement equipment, impactor shape, and test geometry.

Each testing technique has standardized dimensions for the specimens. As our application produces samples of 250 mm in length and 25 mm in width, this method provides two possible standards, ISO 179, and ISO 180 [31,32]. Impact tests are essential to assess mechanical properties such as the resistance of the material, the capacity to absorb the energy, and the corresponding failure modes. The classification is according to the velocity of the procedure (see Table 2-4) [31].

Table 2-4: IT methods with the corresponding velocities

Impact Test	Impact velocity (m/s)	Impact test method
Low velocity	<10	Drop weight Pendulum (Charpy, Izod) Inertia wheel
Medium velocity	10-50	Inertia wheel Servo hydraulic Gas gun
High velocity	50-1000	Gas gun Electromagnetic launcher
Hyper velocity	2000-5000	Light-gas gun Electromagnetic launcher

Currently, there are four types of velocity IT: low-velocity, medium-velocity, high-velocity, and hypervelocity. According to our dimensions, we will be targeted at low-velocity IT, particularly *Charpy testing* (see Figure 2-7) [31], which is outlined inside the pendulum IT.

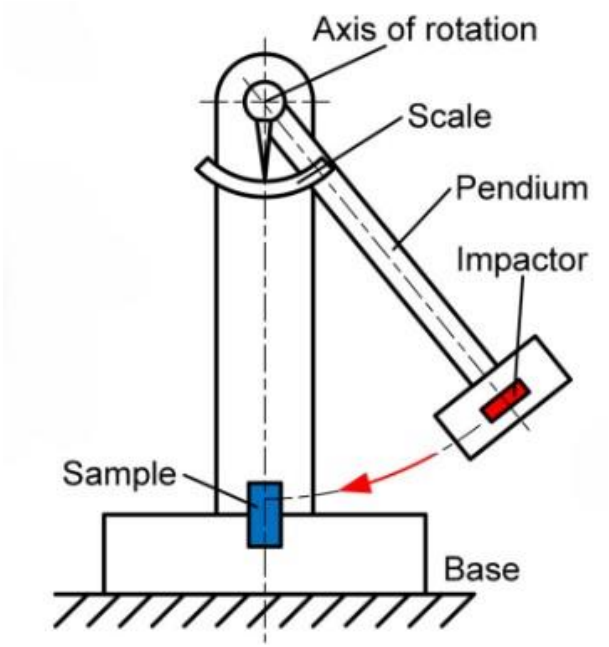

Figure 2-7: Charpy Test

Its main characteristics include a velocity lower than 10 m/s, the specimen standardized dimensions indicated in ISO 179 based on 80 mm in length, 10 mm in width, 4 mm in thickness, and a notch of 45 x 2 mm with a radius of 0.25 mm. It takes advantage of a blunt impactor which allows it to delimit good predictions of forces and failure modes.

After performing, several failure modes can occur. Commonly, low-velocity impact damage is renowned because the material is damaged but used to remain functional to a reduced degree. “Low-velocity impact damage is further subdivided into clearly visible impact damage (CVID) and barely visible impact damage (BVID), with most of the damage occurring in the latter category” (see Figure 2-8) [31].

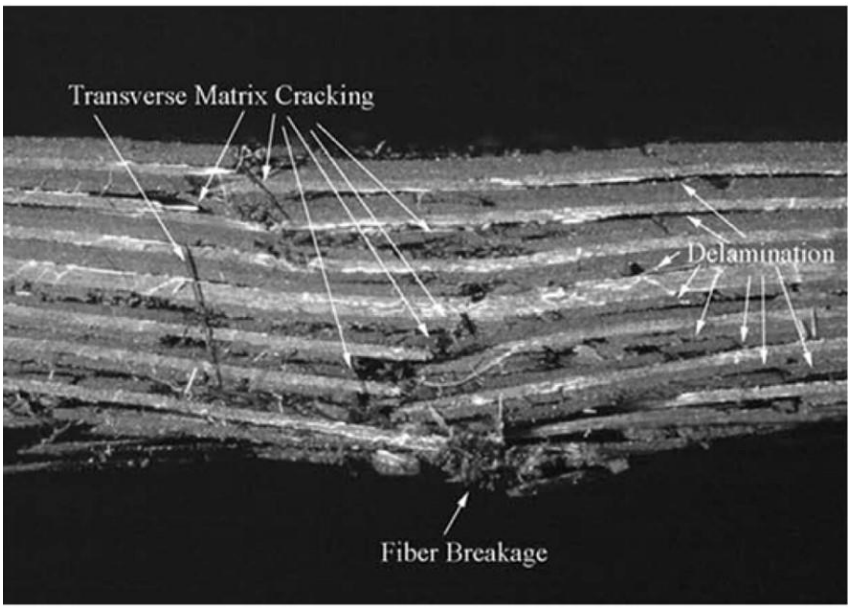

Figure 2-8: Failure modes in low-velocity impact tests

The low-velocity impact test generates matrix microcracks causing delamination, matrix, fiber cracks, debonding, and fiber pull-out. Mechanical properties are negatively influenced by the phenomenon called debonding which affects the matrix and fibers.

2.3.5 Surface Quality Test

The 3D profilometry is one of the most distinguished SQTs in composite materials. These materials are commonly made of woven fibers such as carbon or glass and fixed with an epoxy matrix. To achieve a rigidity structure and aerodynamic parts, carbon fibers are used as light, strong, and moldable materials.

Within the wide field of profilometer machines, the 3D non-contact profilometer (see Figure 2-9) [33], is a good selection since the measurement of the surface is based on axial chromatism. It is relevant to highlight that the test can be done on any size of the specimen with no preparation needed and it has no influence from sample reflectivity or absorption.

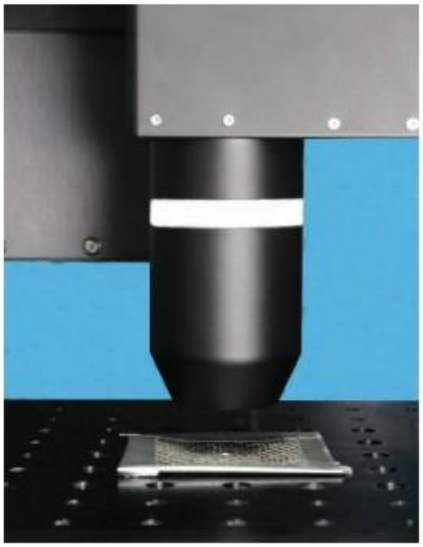

Figure 0-9: Carbon fiber sample being analyzed by a 3D Profilometer

To have a reference of experimental data, two weaves of carbon fiber composites have been measured to assess their surface quality. To characterize these materials, surface roughness, weave length, isotropy, fractal analysis, and other surface parameters need to be determined. The testing is based on selecting a large enough random area that properties can be compared in the surface analysis software.

The main goal is to achieve as strong as possible composite material with a smaller number of defects as feasible. Composites will be in service for a long time, so it is crucial to control the quality of the production. A good procedure to ensure a strong performance over a long service is the profilometry surface inspection.

3 Procedure

This research aims to reach a suitable material for a wing of the support in a hydrofoil surfboard. Reaching this objective involves overcoming three main problems: the environmental impact of greenhouse gas emissions and the handling of end-of-life disposal of cars, reducing the waste of carbon composite fibers, and the variability of the implementation of BMC and SMC processes. Fortunately, as developed in the State of Art, there is a solution to solve these problems. Firstly, the environmental impact is reduced by using the waste of the scrap of the WP. Greenhouse gas emissions are reduced

by using materials as raw materials in new processes. This fact implies that the waste of carbon fibers is reduced, and although getting back the raw materials from finished parts is very energy-intensive, it is offset by recovering the energy lost during the manufacturing process of the raw material. The technological challenge of implementing the BMC and SMC processes is characterized by the variability in the composition of materials and procedures, due to materials do not work the same in both methods. To evaluate the BMC and SMC techniques it is necessary to do the comparison of the different materials made of the different processes. The comparison of the materials does not exist, but it is achieved several standardized possibilities for our application to thoroughly evaluate the plates through the performance of flexural and tensile tests.

The main objective is to compare different plates made of different methods and assess which plate has the best mechanical properties for the application. To evaluate the different composites, it is necessary to assess 2 plates made of BMC, and 2 plates made of SMC. On the one hand, it is disposed of two plates from the Argentinian partner which are made of the BMC technique, and two plates from Toray using the SMC technique. The particularity of these plates not only is the differences in the methods but also the material composition. The composition of the Argentinian partner is not well known because during the manufacture of the plate, fibers were mixed with a certain amount of resin, and after this mixture was mixed again with another amount of resin system, so it is not ensured the quantity of resin that has been used. For this reason, is necessary to manufacture two additional plates with the most similar composition as possible as them, to subsequently evaluate the differences in the behaviors between the six plates. Argentinian plates were made of the BMC process with a press at their facilities. Plates from Toray were made of SMC standard procedure with a press at their facilities. The materials used in both enterprises and for the additional plates are shown in Table 3-1.

Table 3-1: Plates content

PLATE	BASE MATERIAL		BRAND	COMMENT
K1 & K2	Reinforcement		Toray T700SC, 12K, Sizing Type 5 , Tenax-E HTS45 E23 [1]	Long fibers 50-100 mm
	Resin Matrix	Resin	OLIN, DER383, CASRN 25085-99-8 [1]	Mix Ratio (parts by weight): 100:33
		Hardener	HUNTSMAN, Jeffamine D-230, CAS Nr. 9046-10-0 [1]	
	Uncured Scrap		Fiber Volume Ratio of Filament Winding Scrap: 60% [1]	Measured on cured parts
T1 & T2	Reinforcement		Toray T700SC, 12K, Sizing Type 5 [1, 5]	Long fibers around 12.5 mm
	Resin Matrix	Resin	Epoxy for SMC [5]	
		Hardener	-	
	Uncured Scrap		Fiber Volume Ratio of Filament Winding Scrap: 57 % [5]	
L1 & L2	Reinforcement		Tenax-E HTS45 E23 [3]	Long fibers 10 mm
	Resin Matrix	Resin	Elan-Tech EC 14 [2]	Mix Volume Ratio: 100:32 by weight [2]
		Hardener	ELANTAS W 282 [2]	
	Uncured Scrap		Fiber Volume Ratio of Filament Winding Scrap: 54-55 % [4]	

As we can appreciate, although K1 and K2 plates are composed of different materials L and L2 plates are composed of two components. For both laminates, it is used the *EC 14* resin [34], and the *W 282* hardener [35], which form the resin system, and *Tenax-E HTS45 E23* fibers [36].

Before describing the manufacturing procedure for the additional plates, the content of this chapter is defined. Section 3.1 describes the two plate manufacturing procedures and the respective specimens for flexural and tensile tests. In section 3.2 the different tests are defined.

3.1 Production of the plate and specimens

The specific composition of the Argentinian plates is not available, so it is necessary to produce two extra plates with the corresponding composition as similar as possible. Each plate is named with a reference. For the plates from Argentina, it is referred to as K1, and K2 respectively. Plates from Toray are referred to as T1 and T2, and finally, the additional manufactured plates are named L, and L2.

The corresponding plates are made of BMC which are cured with a compression technique, as mentioned in section 2.2. Related to the manufacturing process the sheets are created in TORAY INDUSTRIES, INC partner. The objective is to produce two plates 400 x 400 mm in size with the same composition and procedure as plates 1 and 2 from the Argentinian partner. Before describing the procedure, is essential to designate the necessary materials (see Table 3-2).

Table 3-2: Composition of plates L and L2

Content	Plate L	Plate L2
Fibers (g)	329,12	233,92
Resin (g)	214,67	158,91
Hardener (g)	56,75	42,01

Owing to plates from Argentina having different dimensions from the L, and L2 plates, the corresponding quantities of the matrix resin and the fibers are first calculated according to the quantities in volume, to subsequently obtain the quantities in mass [37].

Due to this work benefits from the scrap of the WP, it is necessary to adapt the length of the fibers to the required for our application. The production of the plates starts with the cutting of fibers. The process employs spools of long fibers to be cut to the required length as it is described in Figure 3-1.

Figure 3-1: Procedure of the cutting fibers

Firstly, the fiber from the spool (see Figure 3-1①) is winded in a rectangular structure as shown in Figure 3-1②. Then both ends of the slab are joined together with a paper tape. The slab is placed in the 2D Cutter Table (see Figure 3-1③). The slab is covered with plastic and the vacuum is actioned to keep all the fibers positioned in the table (see Figure

3-1). Finally, long fibers are cut into 10 mm in length (see Figure 3-1), and picked up to produce the L and L2 plates.

The procedure to produce the new plate is described step by step (see Figure 3-2Figure 3-1).

Figure 3-2: Plate production

The necessary components are shown in Figure 3-2①. The resin is mixed with the hardener. The mixture must be completely uniform, and at that point, some bubbles will appear. Then, the resin system is mixed with the fibers to achieve the paste.

The second step consists of putting the paste into the plastic film inside the square and expanding it to get a uniform template (see Figure 3-2②). To facilitate the expansion of the paste, a roller should be used. Then, this paste is covered with another layer of plastic film. The third step involves covering the plastic film with a peel ply, and the sample is turned so the textile layer is now in the lower part. This layer is used to place the sample in the press machine. Forthwith, the plastic film is peeled off from the sample, so it is covered by the textile layer, and then placed in the machine.

Finally, the paste is compressed by the press, and it starts the curing process. The final product is shown in Figure 3-2③. The respective settings of the compression tool are shown (see Figure 3-2).

Table 3-3: Compression process settings

STAGE	TEMPERATURE [ºC]		FORCE [KN]	TIME [s]
	Zone 1	Zone 2		
1	108	110	505	9900
2	108	110	505	8550
3	250	260	1280	30
4	150	150	2000	30
5	150	150	1500	30
6	150	150	2000	30
7	150	150	3300	30
8	150	150	300	30
9	150	150	3300	30
10	150	150	800	30

The compression procedure is made with a closing speed of 0.5 mm/s. It can be appreciated that the process is divided into 10 stages and 2 zones. It is noticed that during the first two phases, meaning almost all of the process, the temperature adopts a stable value of 108 ºC in the case of zone 1 and 110 ºC in zone 2. It can be considered that although there is a period of 30 seconds in which the temperature increases to 250 ºC in zone 1 and 260ºC in zone 2, the rest of the procedure is carried out at 150ºC. Moreover, during the first two stages, the force takes the value of 505 KN, but the rest of the period oscillates between 300-3300 KN. Ideally, two stages would be enough to be completed, but as the program settings have a maximum value, the rest of the time must be added in more stages of 30 seconds. The procedure lasted 5 hours and 9 minutes.

Related to the production of the specimens. There are six plates with different compositions between them. Each plate receives a name related to its origin, methodology, and composition according to subsection 2.3.3, and as mentioned in Section 3.1.

Two tests are described: FT and TT. Each test requires a minimum of specimens to evaluate a plate. In this case, 7 rectangular specimens for each plate are evaluated. As mentioned in Section 2.3, the dimensions of the specimens according to the respective norms are shown (see Table 3-4). Particularly, the FT is evaluated through the comparison of five laminates, and the TT is evaluated through the comparison of six laminates.

Table 3-4: Dimensions of the specimens

	Plate	Thickness [mm]	Width [mm]	Length [mm]	Span Length [mm]
Flexural Test	K1	2,71	26,71	50	40
	K2	1,92	26,20	50	40
	T1	2,21	25,12	50	40
	T2	3,10	11,22	65	52
	L	3,86	10,05	80	64
Tensile Test	K1	4,84	24,26	250	150,63
	K2	4,67	25,89	250	151,00
	T1	4,52	24,066	250	150,54
	T2	5,51	24,44	250	150,17
	L	5,77	25,52	250	150,58

On the one hand, is essential to highlight that in the FT there is a variability in the dimensions of the specimens because of the thickness. As it is mentioned in the standard DIN EN 14125 [28], if the thickness does not coincide with the standard value, which is 4 mm in this case, the corresponding adaption must be applied. For this reason, K1, K2, T1, and T2 plates needed this correction because they have a lower thickness than the standard. On the other hand, in TT as this research is based on specimens with a random orientation of fibers, the restrictions that are fixed by the standard ASTM D3039 [38], are the width, the length, and the gage length, meaning the thickness is not an influence fact. Due to this, all the specimens have the same dimensions. In this test, the main restriction depends on the orientation of fibers but is not applied to our application.

The TT is evaluated by testing six laminates. The methodology of specimen preparation is described in Figure 3-3Figure 3-3: Preparation of the specimen T2. The following procedure has been repeated with each laminate. To produce the specimens, the following components are required:

- Adhesive mass: 30 g
- Hardener mass: 24 g
- E-glass tabs: 24 tabs of 50 mm in width.

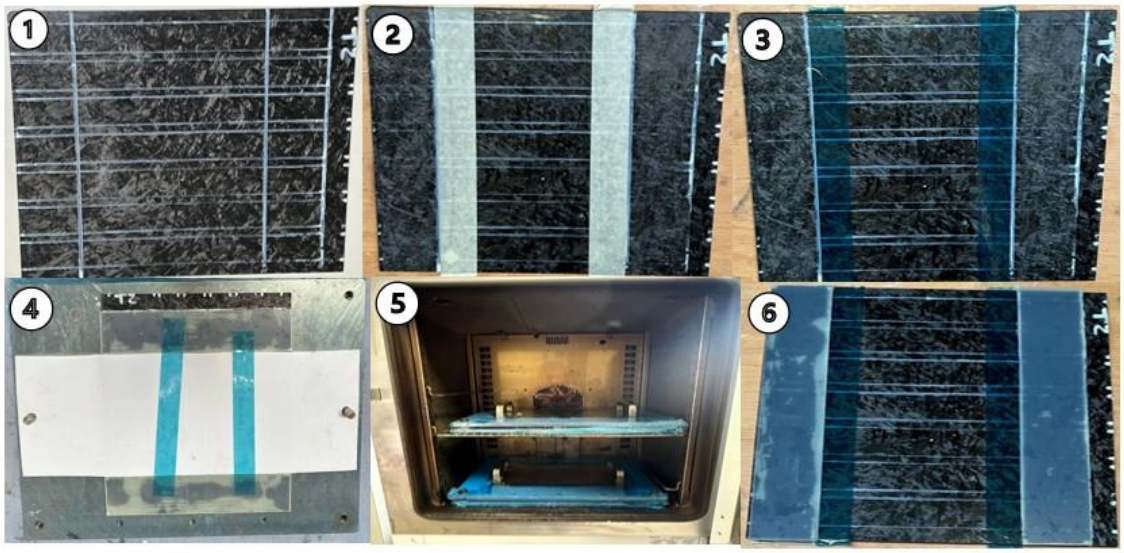

Figure 3-3: Preparation of the specimen T2

All the following steps are going to be repeated on both sides, front and back. The first step is to mark the dimensions mentioned in Section 2.3 of all the specimens (see Figure 3-3 ①). The second step is to sand the area of the tapes. To achieve the appropriate behavior of the material, it is important to take care of the gauge section. For this purpose, the ends of the mentioned section are covered by paper tape to proceed with the sanding process (see Figure 3-3 ②), and the tapes are substituted with flash tape (see Figure 3-3 ③). Then, 5 g of adhesive is mixed with 4 g of hardener to produce the adherent paste. This paste is used to fix the tabs on the laminate which will protect the gripping zone of the specimen. Subsequently, Teflon bands are placed on the gage area and fixed with the blue tape (see Figure 3-3 ④). The laminate is placed on the tool, fixed with the screws, and deposited in the oven for almost 14 hours at 60 ºC (see Figure 3-3 ⑤). Finally, the specimens are ready to be cut (see Figure 3-3 ⑥).

Forthwith the FT procedure is described in Figure 3-4. This process is repeated with each laminate.

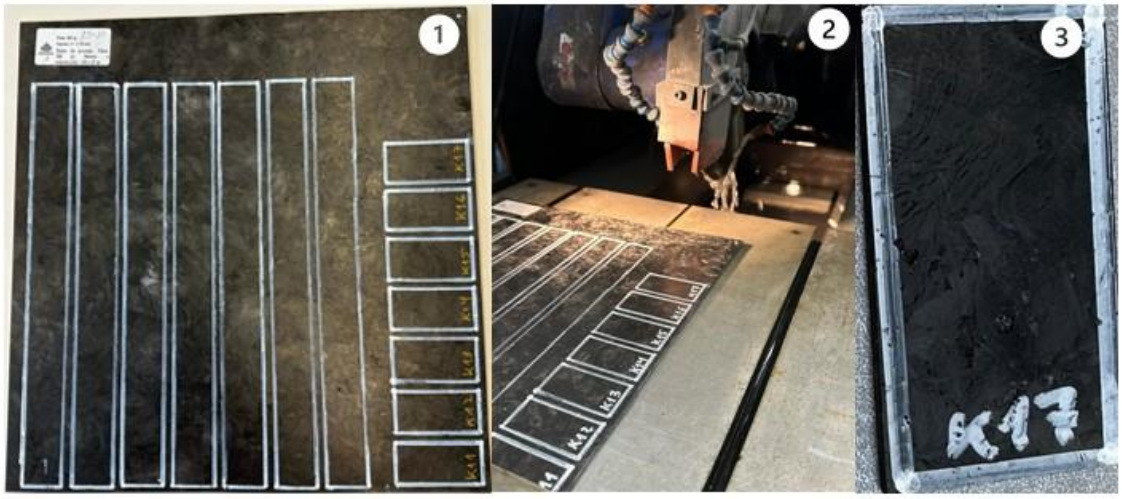

Figure 3-4: Preparation of the specimen K1

The first step is to draw in the corresponding laminates, the standardized dimensions of the specimens as mentioned in Section 2.3 (see Figure 3-4①). The second step is to cut the specimens (see Figure 3-4②). Finally, the specimen is reached successfully (see Figure 3-4③).

3.2 Mechanical Testing

This section describes the test procedure.

3.2.1 Tensile Testing

As shown in Figure 3-5, this test has been carried out through a static electromechanical universal testing machine (Hegewald & Peschke – Inspekt).

Figure 3-5: Static electromechanical universal testing machine (Hegewald & Peschke – Inspekt)

The corresponding procedure starts with the connection of a video extensometer (see Figure 3-6①). It is calibrated through a program that simultaneously is connected to the software LIMESS Messtechnik u. Software GmbH (see Figure 3-6②), according to the gage length of the specimen.

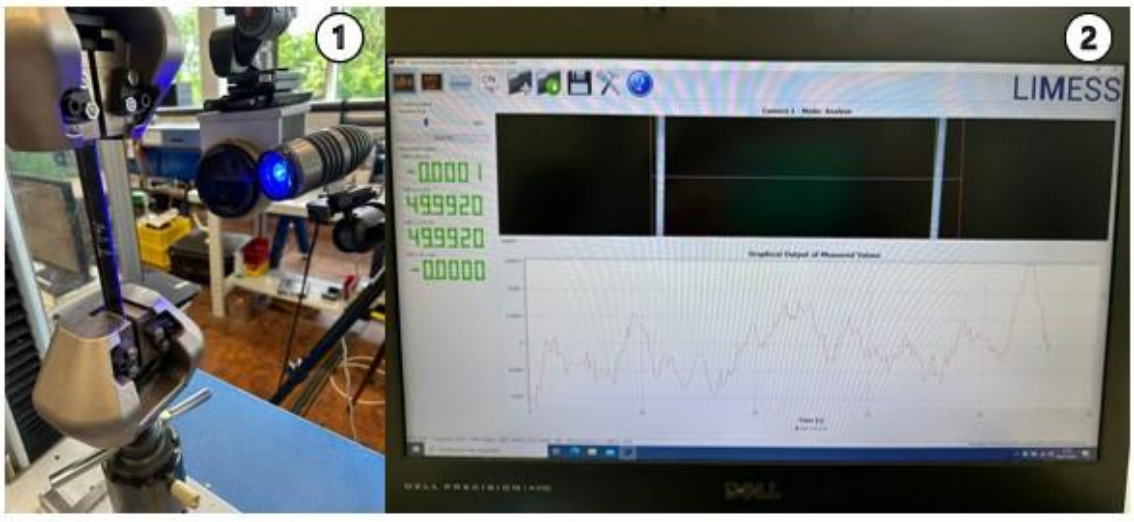

Figure 3-6: 1) Video extensometer, and 2) the respective software

The test starts by calibrating the clamps according to the thickness of the specimens. The first step is to horizontally center the specimen between the two marked lines in the lower and upper clamps and keep it perpendicular to them (see Figure 3-6①).

Additionally, the specimen has a gage length marked with black-white lines that are used as the range length reference for the video extensometer. This side of the specimen and the video extensometer are placed opposite of each other. Straightaway, an increasing force is applied through the clamps until the specimen reaches the fracture. During this test, the cross-sectional area of the specimen remains constant, but the gage length is elongated due to the applied load. The clamps are regulated with a controller that has the same characteristics as the one used in the bending test (see subsection 3.2.1).

3.2.2 Flexural Testing

The UTM is used to realize the three-point flexural test (see Figure 3-7).

Figure 3-7: UTM

During the testing procedure, the software *LabMaster* is applied to connect the machine controller (see Figure 3-8), which displays the settings of the test, with the software.

Figure 3-8: UTM Controller

The first step is to adapt the position between both support pins and the central pin (span length), using the specimen as a reference. The specimen is centered, making sure that the nose is in the middle of the width, length, and span length. Then, adjust the loading nose until the force turns to a value closer to zero. Finally, an increasing force is applied until the fracture appears.

4 Results and Discussion

In this chapter, the results are shown and evaluated, focusing on identifying optimal laminates in terms of performance efficiency and durability. Section 4.1 delves into the outcomes of the tensile test (TT), while Section 4.2 focuses on the results of the flexural test (FT).

4.1 Tensile Test

In this test, six plates made of long fiber-reinforced material are characterized by assessing four main properties: stress-strain curve, UTS, Young's modulus, and stiffness. The calculations for these properties are performed using the equations detailed in subsection 2.3.3 and the data obtained from the LIMESS Messtechnik u. Software GmbH, as referenced in subsection 3.2.2. This data facilitates the derivation of the stress-strain curves presented below. According to the norm ASTM 23039 [23], seven specimens were aimed for the preparation. Therefore at least five viable ones are in the test. Some specimens excluded at various stages are noted in the graphic evaluations. The tested specimens are recorded in Appendix A.

The stress-strain curves for each plate are first described. Afterward, the evaluation of Young's modulus, UTS, and stiffness is taken place. The test groups are organized into three categories:

Group K includes Argentinian plates K1, and K2, manufactured by using the BMC process. Group T comprises T1, and T2 plates, produced using the commercially available SMC process. Group L in this test includes two plates, L1 and L2, produced by using the BMC process. The plate L1 was initially produced, but additionally, another plate named L2 is produced, with specimens named consecutively from L21 to L27. Specimens from each group are numerically identified according to their respective plates. Although detailed composition data is limited for the commercial SMC plates, Table 4-1: Composition of the BMC and SMC platesTable 4-1 shows the composition of the BMC plates (L1, L2, K1, K2), and the SMC plates (T1, T2).

Table 4-1: Composition of the BMC and SMC plates

Plate	Fibers [g]	Resin [g]	Hardener [g]	Total Weight [g]	Thickness	Fiber Ratio (wt%)
L1	329,5	214,7	56,8	601	3,6	54,83%
L2	233,92	158,91	42,01	434,84	2,9	53,79%
K1	204	174,24	46,06	424,3	2,5	48,08%
K2	280,5	239,583	63,333	583,416	2,5	48,08%
T1	-	-	-	-	2,3	57,00%
T2	-	-	-	-	3,35	57,00%

SMC plates present higher fiber ratios at 57%, indicating a significant proportion of fibers relative to the total material weight. This fact suggests a consistent manufacturing process, achieving a high strength-to-ratio. In addition, the thickness of SMC plates varies within a narrow range of 2.3 mm to 3.35 mm. This demonstrates a greater control and uniformity in material properties.

Conversely, BMC plates have more variation in fiber ratios, with a range from 48.08% to 54.83%. BMC plates also present a significant variability in thickness with a range from 2.5 mm to 3.6 mm. This variation indicates that the BMC process may produce less uniform material properties compared to the SMC process.

The first stress-strain curve to be described is related to the plate K1.

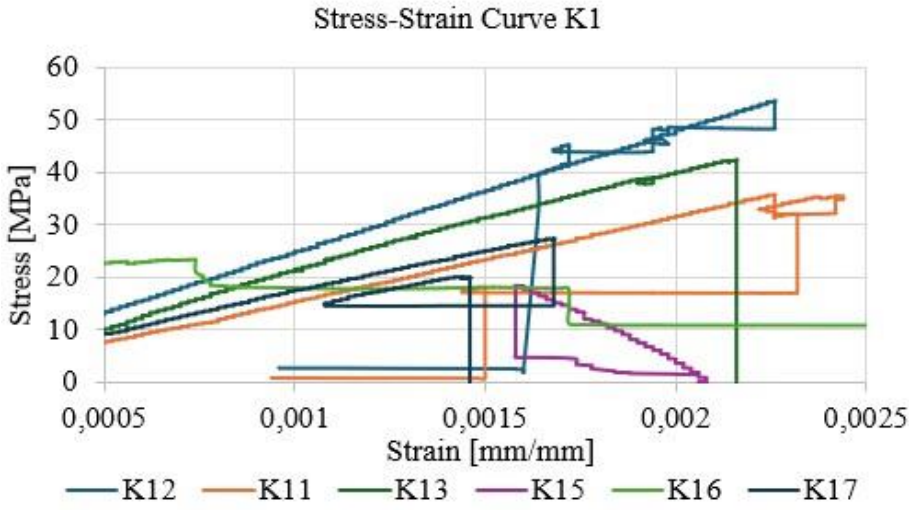

Figure 4-1: Stress-strain curve K1

Afterwards, the stress-strain curve of plate K2 is shown below.

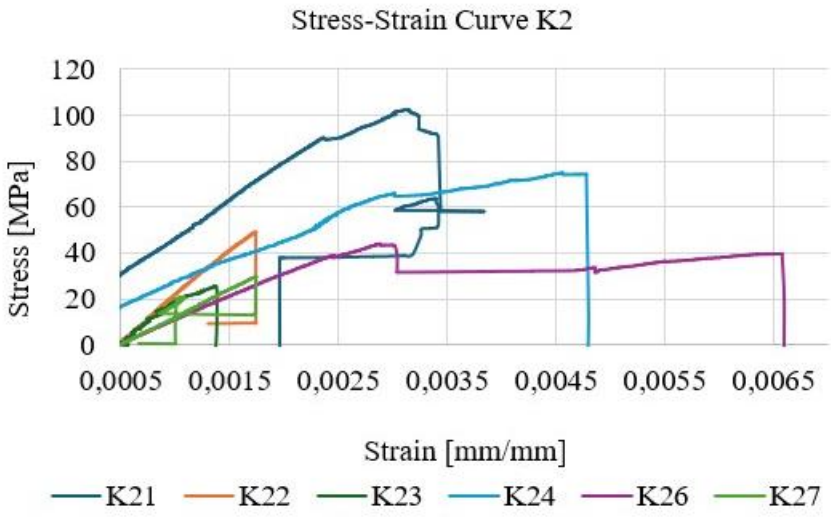

Figure 4-2: Stress-strain curve K2

As observed in Figure 4-1 and Figure 4-2, all the specimens share a similar inclination, conserving the material characteristics.

For specimens K11, K12, K15, and K17 from plate K1, and K21, K22, and K27 from plate K2, the curve shows that after the first peak, the value decreases. This behavior is due to the matrix, which increases the elasticity and causes the material to slip.

Specimens K14 and K25 are not considered for the evaluation due to being out of the strain range. Specimen K14 shows a strain range from 0.0168 mm/mm to 0.01814 mm/mm, starting from a strain 100 times higher than the rest. This can be explained because it was not tared before testing. Specimen K25 was incorrectly calibrated in the clamps and broke before the test, providing no data for the evaluation.

Both failures are shown in Figure 4-3, with the front side on the left, and the back side on the right.

Comparing the stress-strain curves of plates K1, and K2 the conservation of the material characteristics is confirmed as they present the same inclination. Additionally, some specimens experienced slipping. Conversely, others showed a sharp drop at the final fracture, suggesting the brittle nature of the fibers.

Figure 4-3: Specimens K14 and K15 on the front side (left), and the back side (right)

To evaluate the Young's modulus of plates K1 and K2, the respective stress-strain curves are shown respectively.

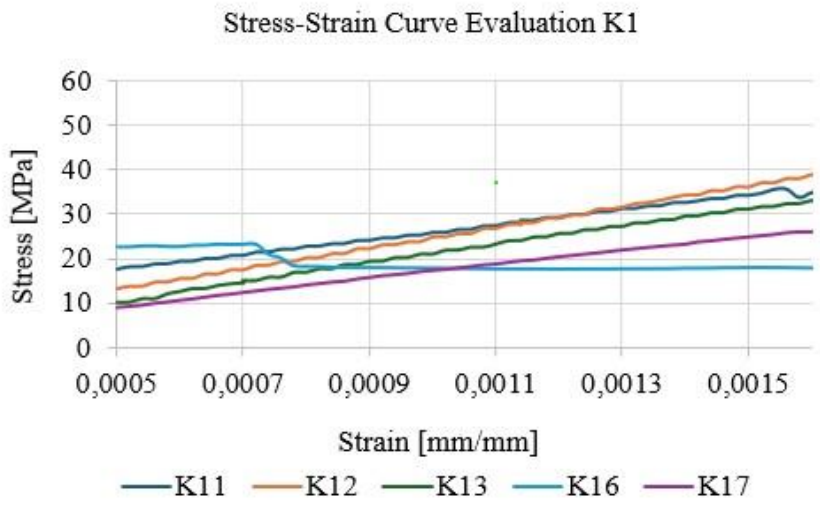

Figure 4-4: Stress-strain curve evaluation K1

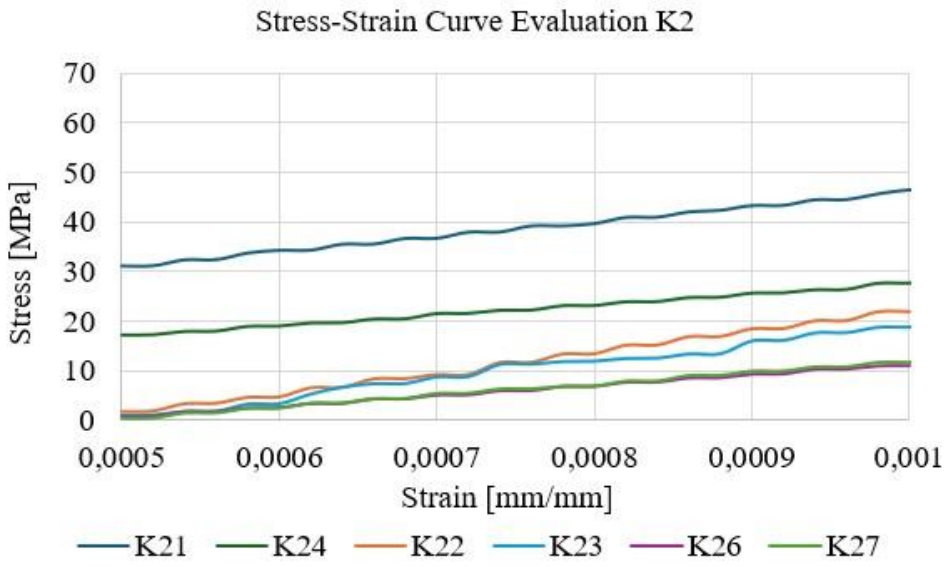

Figure 4-5:Stress-strain curve evaluation K2

As observed in Figure 4-4 and Figure 4-5, oscillations occur because the load cell of the video extensometer does not record elongations accurately, leading to imprecise strain points. With more strain points, these oscillations would be diminished. Another reason for the oscillation is the brittle nature of fibers. Additionally, initial forces cannot be recorded precisely, as forces up to 100 KN are expected.

The initial strain value varies by plate, affecting the evaluation of Young's modulus, and resulting in different strain ranges. For example, plate K1 has a strain range from 0.0005 mm/mm to 0.0017 mm/mm. However, plate K2 has a strain range from 0.0005 mm/mm to 0.001 mm/mm.

Specimen K15 is not considered for Young's modulus evaluation because it is out of the strain range. Specimen K15 shows a decreasing strain range from 0.00208 mm/mm to 0.00194 mm/mm suggesting material slipping.

The stress-strain curves of plates T1 and T2 are shown below.

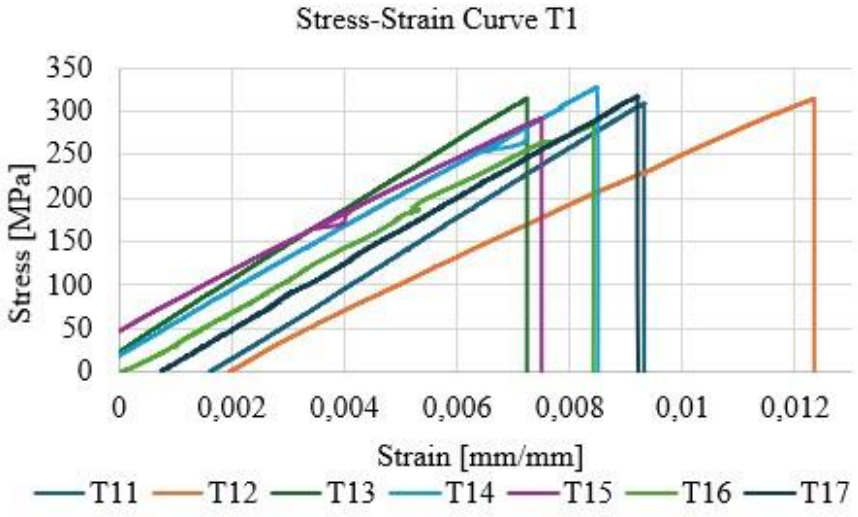

Figure 4-6: Stress-strain curve T1

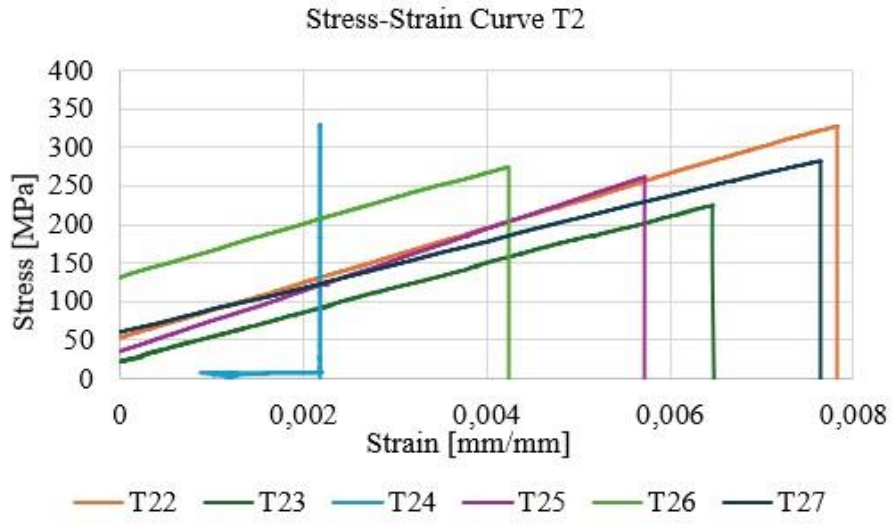

Figure 4-7: Stress-strain curve T2

As observed in Figure 4-6 and Figure 4-7, all the specimens share the same inclination, conserving the material characteristics.

Specimen T21 is not included in the evaluation for two reasons: the video extensometer gage length was not well calibrated, resulting in negative strain data, and the material slipped showing a decreasing strain range from -0.0027 mm/mm to -0.0024 mm/mm. Specimen T24 has a different behavior because, during the test, most of the fibers broke, while some remained intact, causing the load cell to detect the same elongation for increasing loads.

The stress-strain curves for the evaluation of the Young's modulus of plates T1 and T2 are shown below.

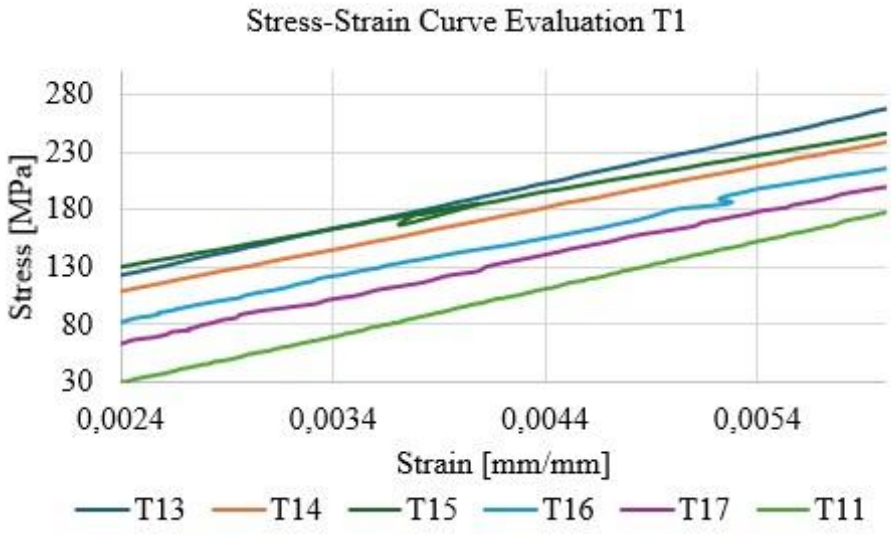

Figure 4-8:Stress-strain curve evaluation T1

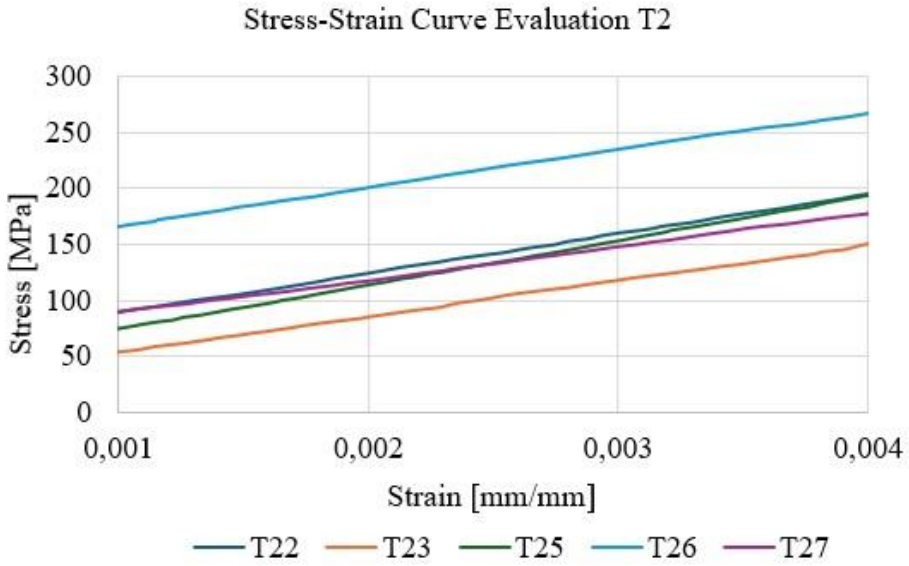

Figure 4-9: Stress-strain curve evaluation T2

As shown in Figure 4-8 and Figure 4-9, plates T1 and T2 show a linear behavior, indicating the preservation of material characteristics and uniformity in elastic properties. Compared to BMC plates, common commercial SMC plates show a more uniform behavior.

Stress-strain curve of plate L1 is provided below.

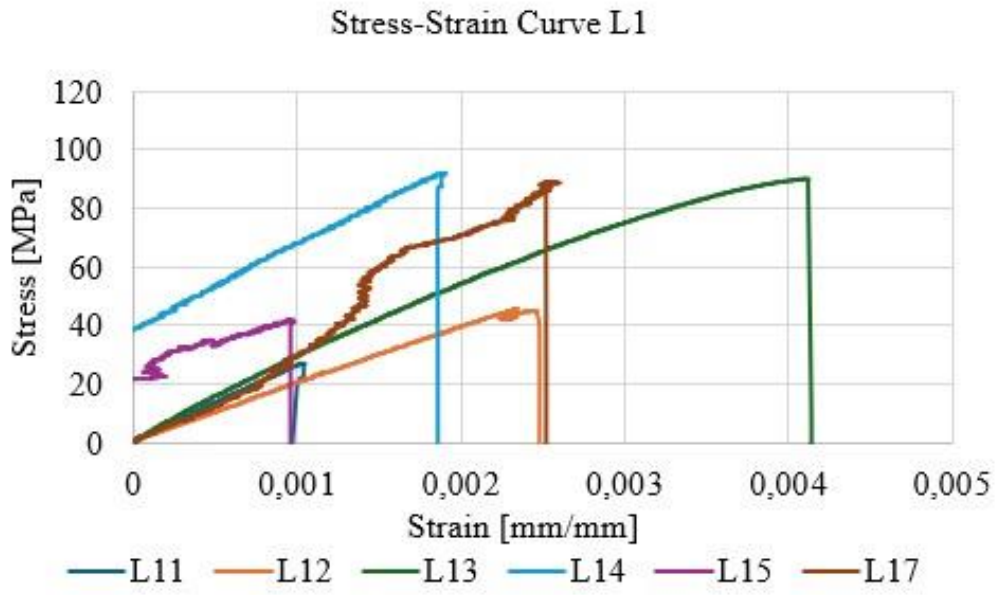

Figure 4-10: Stress-strain curve L1

As observed in Figure 4-10, all the specimens share the same inclination, conserving the material characteristics. Specimen L16 is not considered for the evaluation due to being out of the strain range. The video extensometer gage length was not well calibrated, resulting in negative strain data, and the material slipped showing a decreasing strain range. Specimen L16 has a strain range from -0.00276 mm/mm to -0.00242 mm/mm.

The stress-strain curve evaluation of plate L1 is shown below.

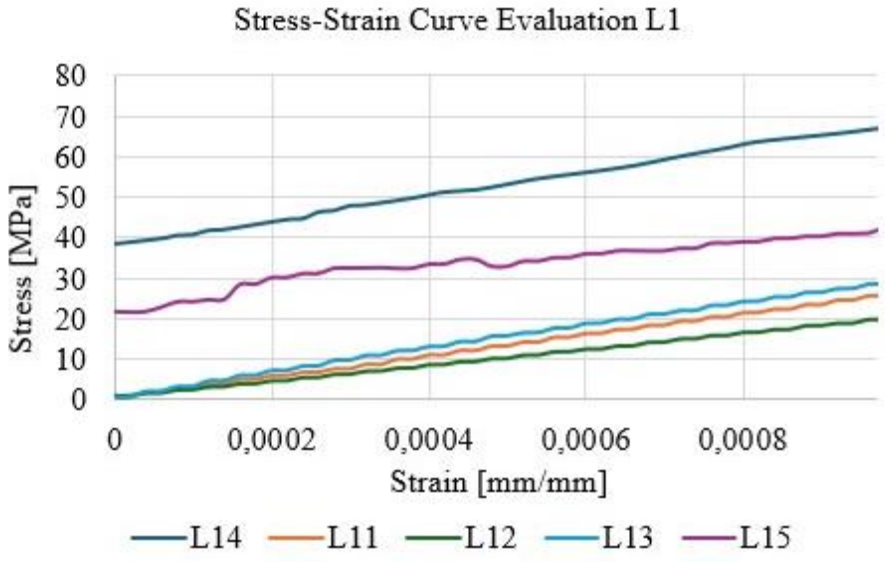

Figure 4-11: Stress-strain curve evaluation L1

As shown in Figure 4-11, the same behavior as in plate K2 is observed. The appearance of oscillations is because the load cell of the video extensometer does not record elongations accurately, leading to imprecise strain points. Another reason for this behavior is the brittle nature of fibers. It is important to consider that plates K2 and L1 have almost the same composition, differing in the fiber ratio. Plate L1 has a higher fiber ratio with a value of 54.83% compared to plate K2 with a value of 48.08%.

The stress-strain curve of plate L2 is provided.

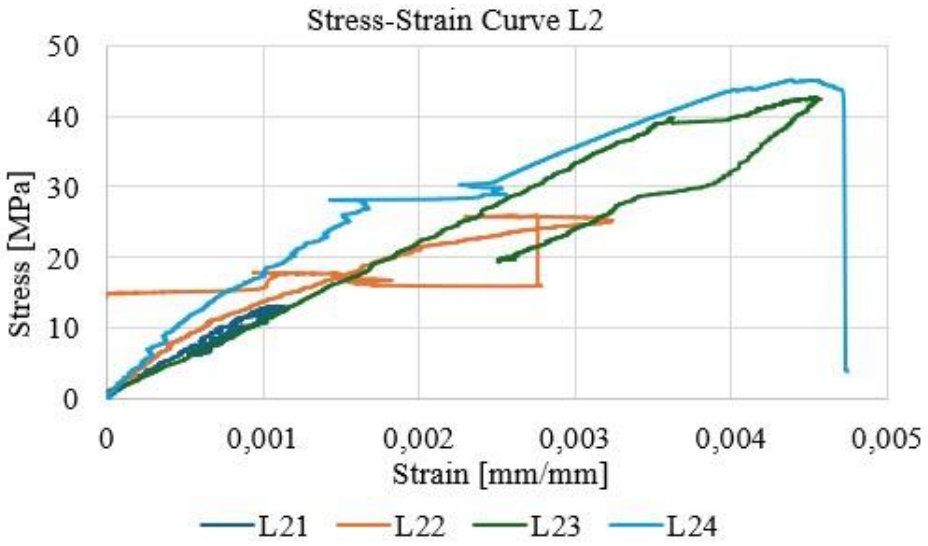

Figure 4-12: Stress-strain curve L2

As observed in Figure 4-12, all the specimens share the same inclination, conserving the material characteristics. This plate contains several uncured parts, as some areas of the plate remain wet. During the production of the plate, the remaining fibers in the fiber container were mixed with the remaining matrix resin. Afterward, all these fibers were mixed with the matrix resin corresponding to the composition of the plate. Consequently, the resin matrix did not cure properly, explaining the decreasing values. Specimens L21, L22, and L23 show evidence of material splitting.

Specimens L25 and L27 are not included in the evaluation due to being out of stress range. Specimen L25 has a stress range from 0 MPa to a maximum stress of 3.1435 MPa. Specimen L27 has a stress range from 0.01241 MPa to a maximum of 0.05957 MPa. These stress values are considered insignificant given the expected 100 KN forces.

Specimen L26 is not considered for the evaluation due to its negative strain range from -0.00002 mm/mm to -0.00366 mm/mm.

A better evaluation of Young's modulus is achieved with a wide range of strain points. To obtain more accurate E values, the assessment is divided into two stress-strain curve evaluations. The first part evaluates the E values of specimens L21, L22, L23, and L24. The second part assesses the L23 and L24. This approach allows for comparing Young's modulus obtained for L23 and L24 in both assessments and evaluating the differences between the results.

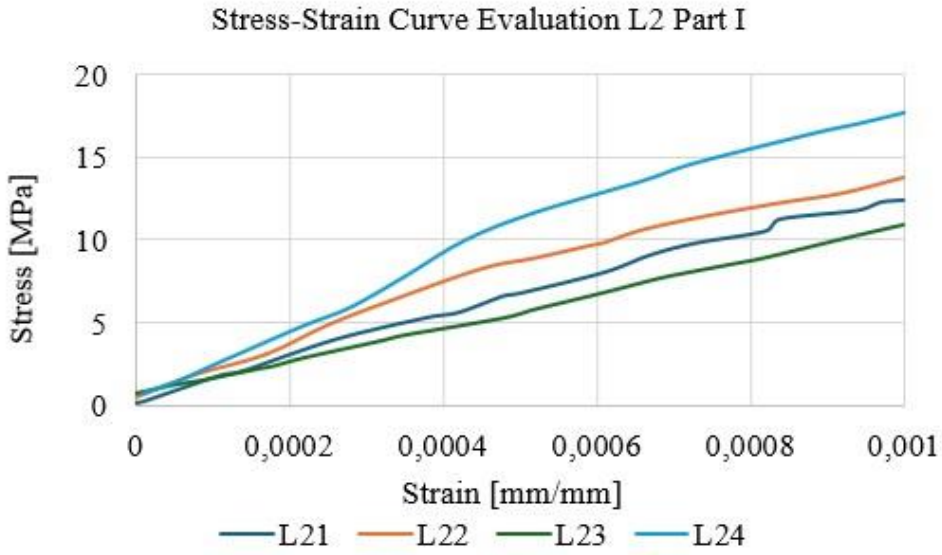

Figure 4-13: Stress-strain curve evaluation L2 Part I

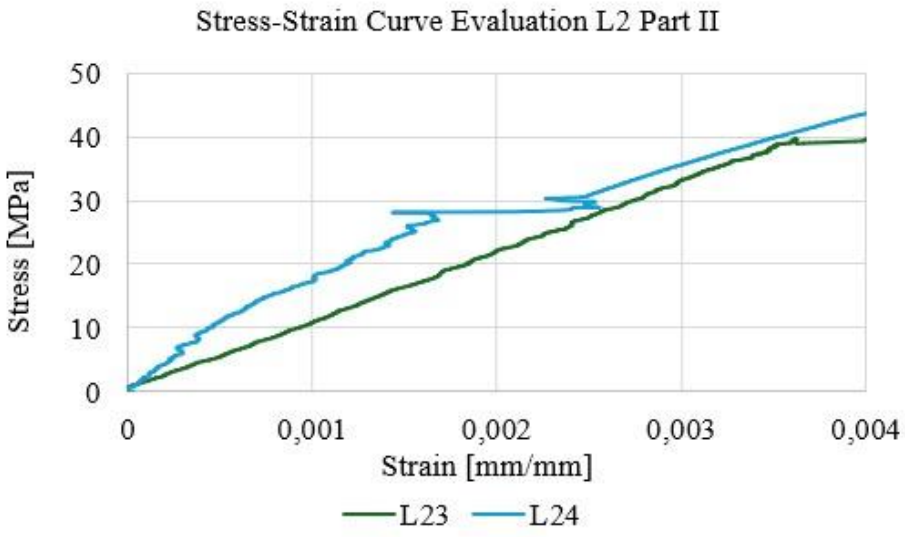

Figure 4-14: Stress-strain curve evaluation L2 Part II

As observed in Figure 4-13, all the specimens share the same inclination, conserving the material characteristics. Figure 4-14 demonstrates that a wider range of strain points reveals greater differences between specimen curves. Although the composition of plate L2 is similar to plate K1, it is observed that for the same difference between the two end strain points, plate K1 shows a stress difference of almost 30 MPa. However, plate L2 shows a stress difference of almost 20 MPa for the same strain point difference.

Figure 4-15 show several wet areas of specimens from plate L2.

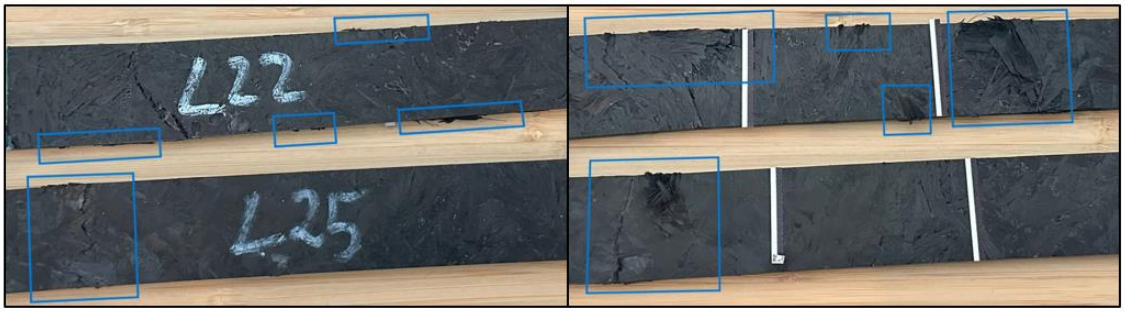

Figure 4-15: Specimens L22 and L25 on the front side (left), and the back side (right)

As mentioned in the previous stress-strain curves, some specimens are not included in the average Young's modulus. Forthwith Young's modulus and stiffness are demonstrated in Figure 4-16, and Figure 4-17.

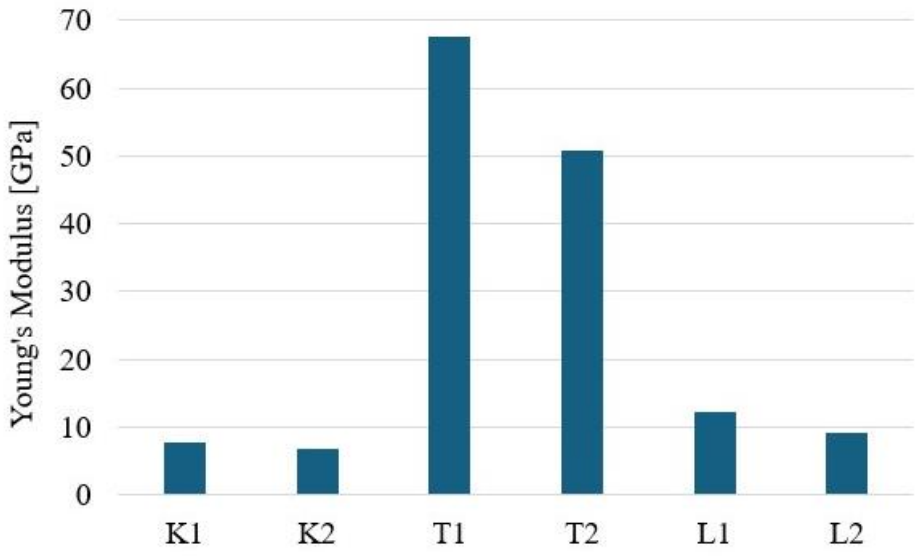

Figure 4-16: Mean Young's modulus of each plate

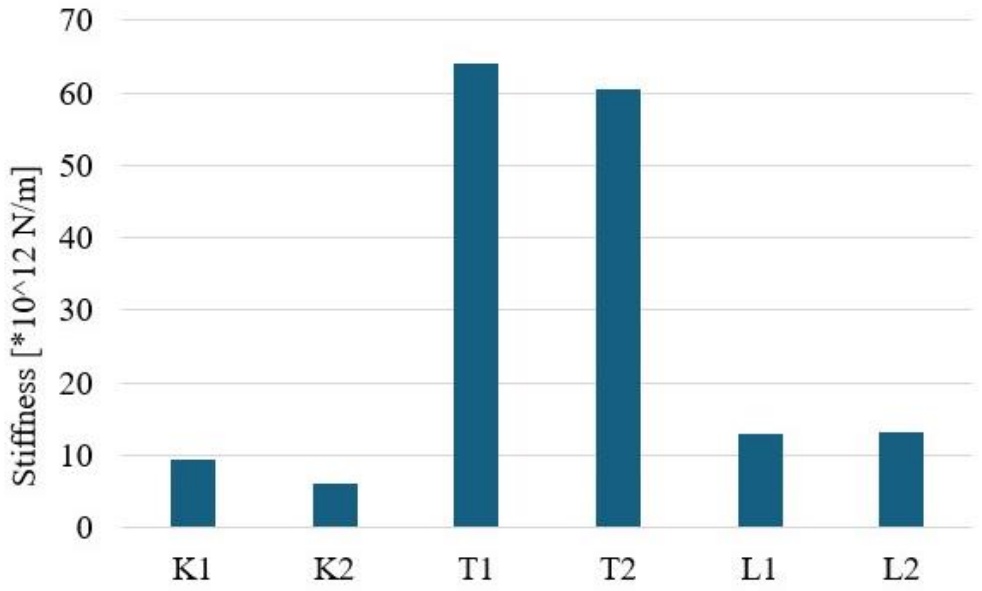

Figure 4-17: Mean stiffness of each plate

This test aims to compare the different combinations of the corresponding plates. Initially, a specific comparison is conducted. Forthwith a general evaluation is carried out. For this assessment, two points are considered: the methodology and the composition, including the fiber ratio and the resin matrix.

The test results show that the plates T1 and T2 have the highest Young's modulus values, with T1 at 67.6971 GPa and T2 at 50.8887 GPa. Among the BMC plates, plate L1 possesses the highest Young's modulus with a value of 12.301 GPa.

The fiber ratio scale aligns with Young's modulus order. Plates T1 and T2 have a fiber ratio of almost 57% [5]. Plates L1 and L2 have a fiber ratio of 54.83%, and finally, plates K1, and K2 have a fiber ratio of 48.08% (see Table 4-2).

L plates are produced using K plates as a reference, thus comparing their corresponding composition. According to the comparison between plates L1, and K2. Plate L1 with a Young's modulus of 12.301 GPa, is 80.35% higher than the E value of K2 of 6.8155 GPa. This difference is due to the higher matrix content in K2 and its lower fiber content. Consequently, the stiffness from plate L1 with a value of $13.0095 \cdot 10^{12}$N/m, is 116.62% higher than plate a stiffness value of K2 of $6.0062 \cdot 10^{12}$N/m.

Comparing plates L2 and K1, it can be appreciated that the same pattern as the previous evaluation is given. Plate L2 Young's modulus is 18.74% higher than plate K1. The

results can be influenced by the plate L2 since it was not cured enough. Additionally, L2 possesses a 38.5% higher value in stiffness than plate K1.

Finally, all the different composite materials are compared. It is concluded that SMC materials, considering that contain endless fibers, are the optimal option for our application. Plates T1 and T2 contain on average 55.6% in Young's modulus and 498.3% in stiffness higher than the BMC plates with a value of $64.0714 \cdot 10^{12}$ N/m for plate T1, and $60.4998 \cdot 10^{12}$ N/m for the plate T2, meaning almost five times the values achieved with BMC materials. Conversely, although BMC materials have lower values compared to SMC materials, plate L1 could be a good selection depending on the application requirements.

The Ultimate Tensile Strength (UTS) is shown below.

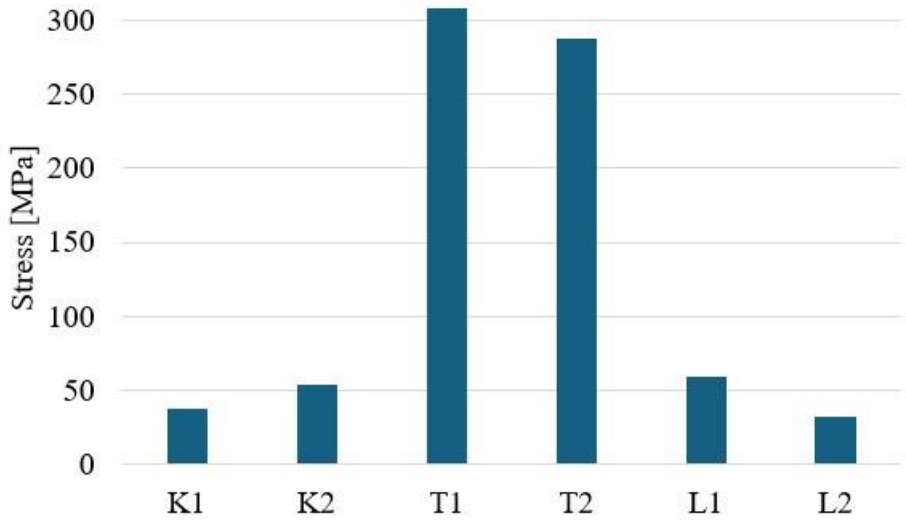

Figure 4-18: Mean ultimate tensile strength (UTS) of each plate

To evaluate the maximum load that the material can support, the UTS is assessed. Comparing the BMC plates, it is concluded that there is not a significant difference between the plates evaluated in the thesis. For instance, plate L1 with a value of 58.5801 MPa has a UTS of 8.2% higher than plate K2, with a value of 54.1427 MPa. However, in this case, K1, with a value of 37.1627 MPa is 17.5% higher than in plate L2, with a value of 31.6262 MPa. Finally, there is a relevant difference between the SMC plates and the BMC plates. On average, SMC plates have UTS values 556.6% higher than the BMC materials, more than five times higher than BMC plates. This is due to the manufacturing methods. In the BMC method, fibers are mixed with the resin matrix randomly.

Conversely, in the SMC method, fibers are spread through a conveyor belt, ensuring that the number of fibers in each part of the plate is almost equal, unlike the BMC process.

4.2 Flexural Test

In this test, five composite materials are characterized by determining three main properties: stress-strain curve, UTS, and Young's modulus. These properties are calculated according to the respective equations as mentioned in subsection 2.3.3. The tested specimens are recorded in Appendix B. Forthwith, the stress-strain curves are provided. Each graphic contains several curves, representing the specimen behavior. According to the norm DIN EN 14125 [2], seven specimens were aimed for the preparation, therefore at least five viable ones are in the test.

The test samples are categorized into three groups: K, T, and L. The K group includes both Argentinian plates K1, and K2, produced by using the BMC. The T group comprises T1, and T2 plates, produced by using the commercially available SMC process. Finally, the L group consists of a single plate made by the BMC process. The specimens are numerically identified according to their respective plates. For instance, since there are 7 specimens from each plate, plate K2 will contain the specimens consecutively named from K21 to K27.

A preliminary review highlights the observed failure modes: ductile and brittle. The brittle failure is characterized by a rapid crack propagation initiated at existing flaws, resulting in an abrupt material failure. Conversely, the ductile failure is based on a gradual damage accumulation, visible as a steady decline in the stress-strain curve. Although the composite materials principally exhibit brittle characteristics due to fiber cracking, areas with higher resin content may show ductile behavior. This analysis is crucial for assessing the structural integrity and suitability of each tested composite material.

The stress-strain curves of plates K1 and K2 are shown below.

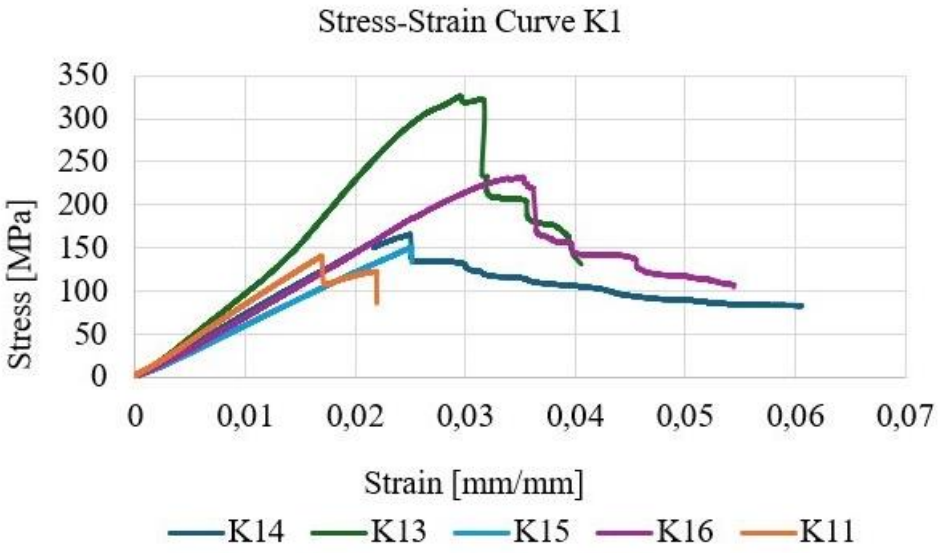

Figure 4-19: Stress-strain curve K1

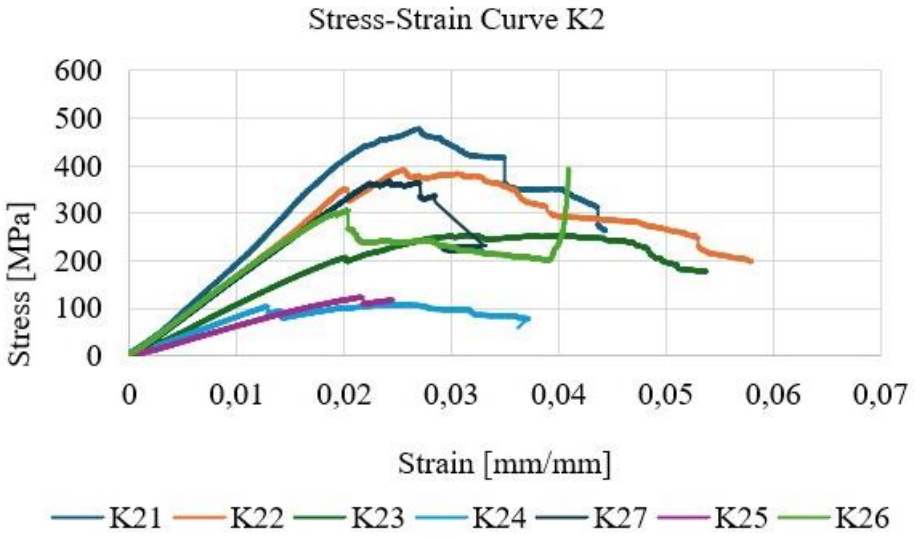

Figure 4-20: Stress-strain curve K2

Figure 4-19 and Figure 4-20, show the stress-strain curves of plates K1, and K2. There is a significant variability in the behavior of the composite materials. Although both plates contain the same percentage of resin of 0.41% and fibers of 0.48% [3], plate K2 can support higher loads under the same conditions.

In plate K1, specimens K11, and K15, show that the final stress value is proportional to the initial peak. The failure is produced when the stress value reaches 80% of the initial peak. However, specimen K14 exhibits a gradual decline after the first peak. Finally, specimens K13, and K16, reach failure through abrupt drops after their initial peaks.

In plate K2, specimens K21, and K22 experience gradual declines after their peaks. Conversely, specimens K23, K24, and K27 show sharp drops in their stress-strain curves after their peaks.

The stress-strain curves of plates T1 and T2 are provided.

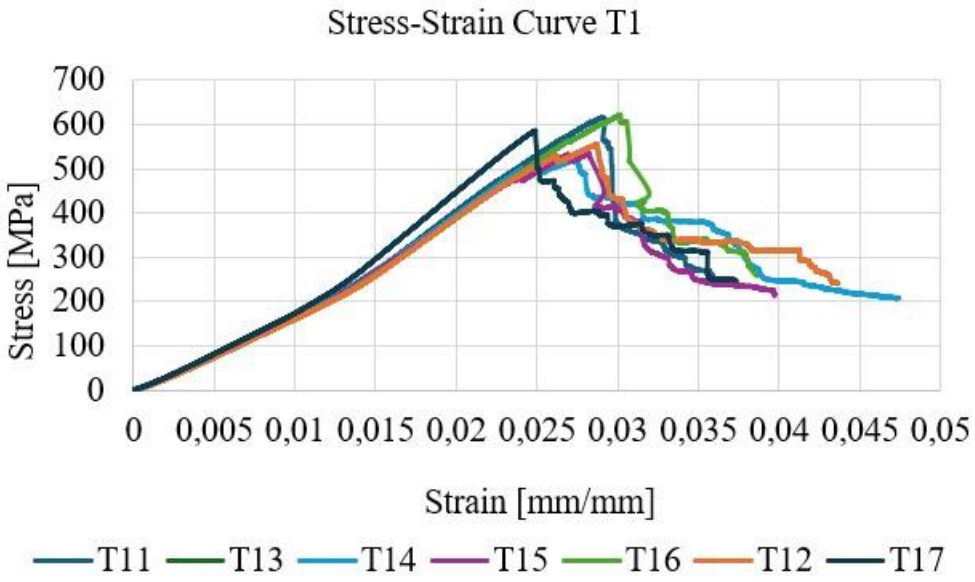

Figure 4-21: Stress-strain curve T1

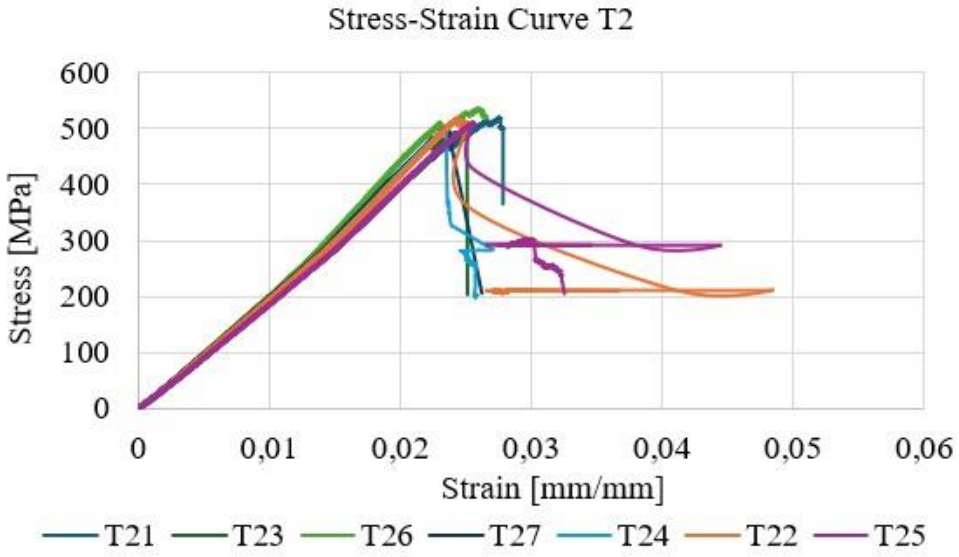

Figure 4-22: Stress-strain curve T2

Figure 4-21 and Figure 4-22 illustrate the behavior of the plates T1 and T2. Specimens from plate T1, absorb more energy and support higher loads compared to those in the T2 group. Different from T2 specimens, which demonstrate a relatively proportional decline after the initial peak, the T1 group is characterized by several abrupt drops. Generally, all the specimens within each plate show similar behavior, sharing the same inclination which suggests that they conserve the material characteristics.

Forthwith, the stress-strain curve of plate L is shown.

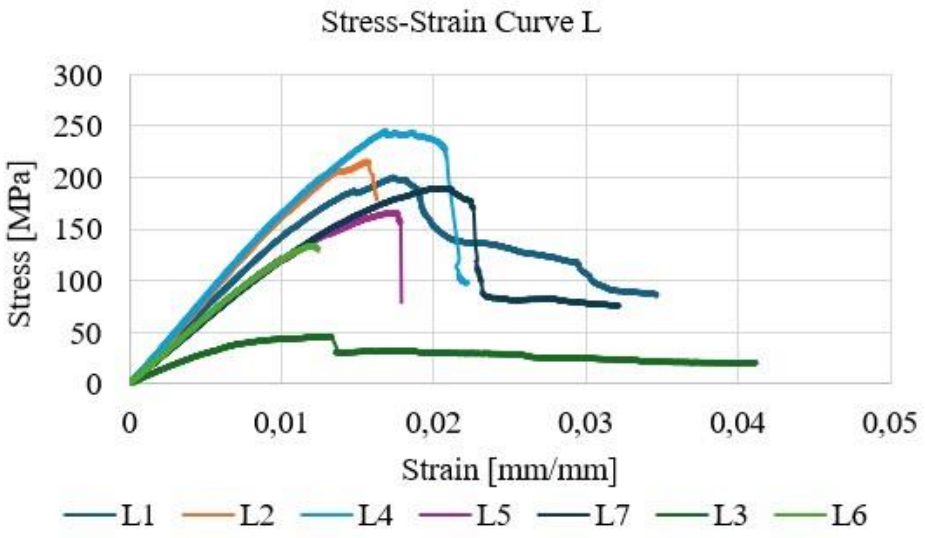

Figure 4-23: Stress-strain curve L

As shown in Figure 4-5, except for specimen L1, all the specimens in plate L exhibit a similar behavior characterized by an abrupt drop. Plate L contains some areas with irregular surfaces, meaning that there was a higher number of fibers on them.

After describing the stress-strain curves, Young's modulus is evaluated in detail in Figure 4-24, Figure 4-25, and Figure 4-26.

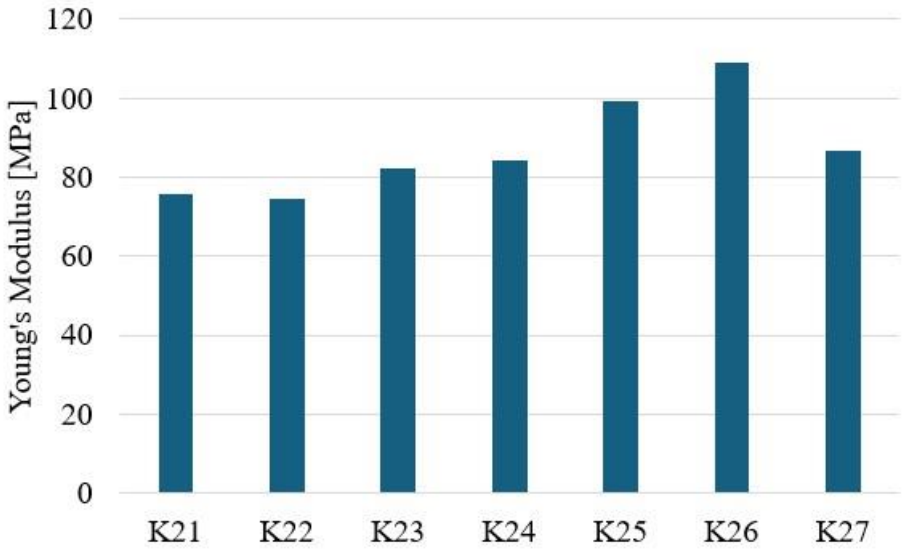

Figure 4-24: Young's modulus of each specimen of plate K2

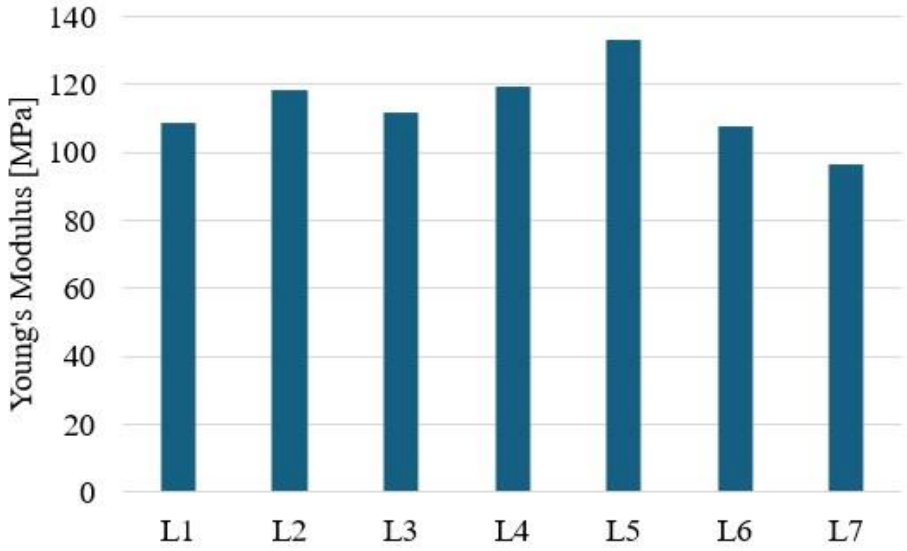

Figure 4-25: Young's modulus of each specimen from plate L

The variability of Young's modulus between plates made by using the BMC process specifically plates K2 and L, is highlighted. This comparison reveals the differences between both plates by using the same technique. Although plate L is intended to have a similar composition to plate K2, notable differences exist. Firstly, during the production of the Argentinian plate, the fibers from the scrap of the WP that were used to produce the plate were mixed with a matrix resin. Afterward, this mixture was mixed with a matrix resin to produce the plate. This fact influences the final composition. Table 4-2 details the base material composition of plates L, and K2.

Table 4-2: Composition of the of base materials of the BMC plates

Plate	Fibers [g]	Resin [g]	Hardener [g]	Total Weight [g]	Thickness	Fiber Ratio (wt%)
L1	329,5	214,7	56,8	601	3,6	54,83%
K2	280,5	239,583	63,333	583,416	2,5	48,08%

As shown in Table 4-2, both plates have more variation in fiber ratios, with a range from 48.08% to 54.83%. Plates L1 and K2 also present a significant variability in thickness with a range from 2.5 mm in the case of plate L1 to 3.6 mm in the case of plate K2. This variation indicates that some differences in the uniformity of the material can appear between both plates.

The mean Young's modulus of each plate is presented.

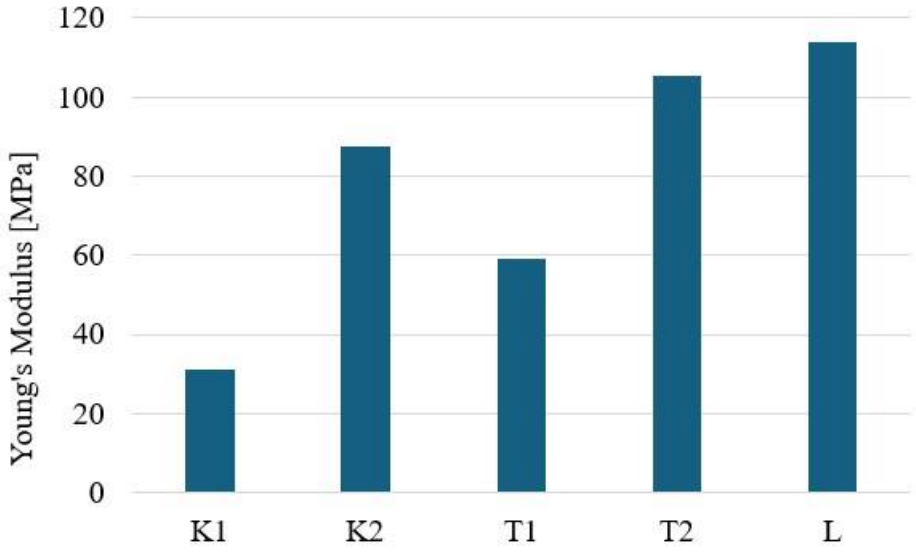

Figure 4-26: Mean Young's modulus of each plate

After analyzing Figure 4-26, plate T2 is worthy of consideration since achieves similar values compared to those of the plate L. Both plates, T1 and T2, produced by Toray have a fiber ratio of 57%. Although this value is the highest, plate L achieves superior Young's modulus values by using fibers from the scrap of the WP and the BMC process. The methodology employed significantly influences these outcomes. In the BMC process, fibers are mixed randomly with the resin matrix. Conversely, in the commercially available SMC, fibers are spread across a conveyor belt, ensuring a uniform distribution across the plate. This uniformity is absent in the BMC process. This fact leads to the appearance of some areas that contain a higher concentration of fibers within the BMC,

enhancing a higher capacity to support loads. This is due to the random orientation of fibers, which are continuously exerting force on the other fibers until failure, in contrast to the more structured arrangement in the SMC process.

The UTS of the specimens of each plate is shown below.

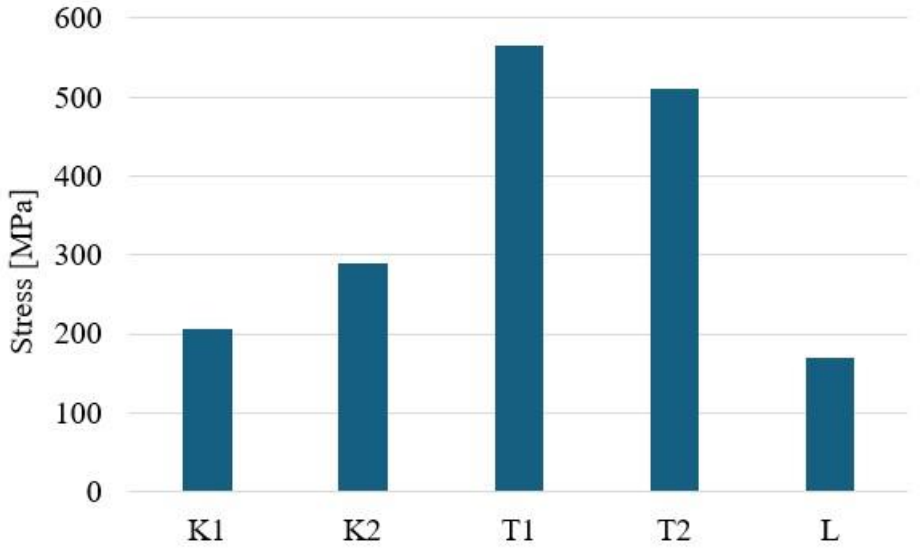

Figure 4-27: Mean ultimate tensile strength (UTS) of each plate

After comparing the capacities of supporting loads of different plates, SMC materials demonstrate a higher capacity to support loads. As shown in Figure 4-27, on average, standard commercially available SMC plates with a value of 538.1634 MPa can support 175.2% more than BMC plates, with a value of 221.0205 MPa.

The mechanical property results of the carbon composite specimens reveal a significant variability. Plate T2 is outlined by possessing high strength, exhibiting the highest values of Young's modulus and UTS. It can be considered the most suitable choice for the demanded application. Moreover, plate T1 also demonstrates having the highest UTS values, indicating its capability to withstand substantial stresses before failing. Conversely, the K1 group of specimens obtained the lowest values in both properties, suggesting its inadequacy for high-stress applications.

Plate L, despite not achieving the highest UTS, records the best Young's modulus values. This performance is attributed to its composition, which incorporates the scrap from the WP used as raw material, influencing its lower tensile load capacity. However, the use of the BMC process, which involves random fiber orientation, enhances its ability to

elongate under increasing force, compensating for some of the weaknesses of the materials.

5 Summary and Outlook

This thesis focuses on developing a suitable material for a hydrofoil surfboard by evaluating BMC and SMC materials. They are characterized by being made of long fiber reinforcement. The primary aim is to compare the mechanical characteristics of different material combinations, specifically evaluating the potential of BMC material against the industrially available SMC material.

The assessment of these materials involves the comparison of six different combinations, each represented by a plate with a defined composition. Two partners, KOHLENIA S. A., and TORAY INDUSTRIES INC, contributed to this evaluation. KOHLENIA S. A. produced two plates using the BMC process with carbon fibers from the WP waste. Conversely, TORAY INDUSTRIES INC used the SMC process to produce two more plates. The BMC plates from KOHLENIA have incomplete composition data since the fibers that were used to produce the plate were mixed with a matrix resin. Afterward, this mixture was mixed with a matrix resin to produce the plate. For this reason, two additional BMC plates were produced from the beginning using the known composition of the Argentinian plates as a reference.

Finally, the variability between BMC and SMC materials is assessed through tensile and flexural tests. Five plates (K1, K2, T1, T2, L), are evaluated in the flexural test, while six plates (K1, K2, T1, T2, L1, L2) are tested in the tensile test. Plate L1 is the same as the plate L used in the flexural test but renamed to differentiate it from the second produced plate named L2.

The production of the new BMC plates started by cutting the fibers through a winding system and a 2D Cutter Table (see section 3.1). The fibers were then mixed with the resin matrix to form a paste, which was spread into a square form and cured. During the production of the plate, some defects, such as irregular surfaces with higher fiber concentration, were noted in plate L. An example is recorded in Appendix A1. Once the plates were ready, the specimens were prepared to start the testing procedure. The

preparation of the specimens was performed according to the norm DIN EN 14125 [28] for the flexural tests, and the ASTM D3039 [23] for the tensile tests (see section 3.1).

Tensile test results indicate that commercially available SMC material remains the best option for supporting higher loads. This is due to they have obtained the higher UTS of all the tests, with an average value of 297.9638 MPa, compared to BMC plates, with a value of 45.3779 MPa. The stress-strain curves show a significant variability in composite material behavior, involving significant challenges in standardizing the test procedure [39]. Plate L2 showed uncured areas, leading to a lower performance during the test. Some examples are recorded in Appendix B1, and section 4.2. This issue was given due to before realizing the mixing of the fibers with the matrix, the container of fibers already contained some remaining matrix. In addition, a proper calibration of the video extensometer gauge length and the static electromechanical UTM is crucial. The consequence of not calibrating properly the specimen in the clamps, being perpendicular to the grip and centered horizontally with the marked lines can produce a decreasing strain and the early failure of the specimen. This fact suggests the slipping of the material. In this case, the test should be repeated. This fact involves that it cannot be considered for the stress-strain curves, and consequently, for the rest of the evaluation. To avoid this, it is recommended to check that the specimen is well placed and that the video extensometer field of view is slightly higher than 50 mm or the closest to it.

The results of the flexural test indicate that the SMC plates withstood on average the highest strength outcomes, with values up to 538.1634 MPa compared to BMC plates with a value of 221.0205 MPa. This is because the BMC plates are composed of wet fibers from the scrap of the wet WP, which can support lower loads. Although plate L does not achieve the highest UTS, it shows the highest Young's modulus values. This fact can be explained because of the entangled fibers from the WP scrap and the BMC process's ability to elongate under force by randomly orienting the fibers. The stress-strain curves reveal a significant variability in the BMC material behavior.

In conclusion, for applications continuously supporting considerable stresses for long periods, selecting a material with a higher Young's modulus is advisable. Plate L, produced from the beginning with the BMC process and composed of recycled fibers, achieves a high modulus of elasticity, making it a suitable choice.

Conversely, for parts subjected to high loads for shorter durations, plate T1 is an astute option. The SMC plate T1 has achieved the highest UTS value of 566.2562 MPa,

compared to the highest BMC plate value of 288.6499 MPa. For long-term load applications, plate L remains the most suitable selection due to its highest Young's modulus value of 113.6846 MPa, comparable to the highest SMC plate value of 105.1584 MPa.

Our application requires high UTS, Young's modulus, and stiffness values to ensure it can withstand substantial loads without reaching failure. Therefore, plates K2, T2, and L are considered the most suitable selections. Plates L and L2 were produced for direct comparison with the Argentinian results. Plates K2 and L are also compared directly, as plate L was produced using plate K2 as a reference. Although the compositions of plates K2 and L are not identical due to variations in the amount of resin and fibers remaining stuck in the mixing container and on the plastic foil, similar results are expected.

In the tensile evaluation, plates K2 and L exhibit similar UTS results, with K2 at 54.1427, and L at 58.5801 MPa. However, they differ in Young's modulus and stiffness, due to plate L double both values of plate K2. Plate L has a Young's modulus of 12.3009 GPa and a stiffness of $13.0096 \cdot 10^{12}$ N/m. In contrast, plate K2 has a Young's modulus of 6.8155 GPa, and a stiffness of $6.0062 \cdot 10^{12}$N/m. These results are compared with the current available BMC results of the plates with a similar fiber ratio (48%) [40]. Both plates show higher Young's modulus and stiffness values, but lower UTS values. The currently available plates average 3.765 GPa in Young's modulus, 63.225 MPa in UTS, and $8.775 \cdot 10^{12}$ N/m in stiffness [40]. The results obtained from plates K2 and L indicate better overall characteristics than the current plates.

In terms of Young's modulus, the different composite materials demonstrate better flexural properties than tensile characteristics, with higher results in the flexural test. However, the materials support higher tensile loads than flexural loads, resulting in higher UTS values in the tensile test compared to the flexural test.

After evaluating the test outcomes, it is interesting to further investigate three aspects: the influence of the temperature during the curing process, the closing speed before curing, and the fiber orientation and defect formation. The curing temperature affects the degree of polymerization, residual stresses, and fiber distribution within the matrix. The closing speed before the curing process impacts the final properties of the composite material. Faster closing speeds can lead to void content, resulting in defects and the reduction of mechanical properties. Finally, fiber orientation is crucial, as the random orientation of

fibers can cause variations in strength and stiffness, as observed in the comparison of the current results [40]. Investigating the correlation between fiber orientation and defect formation can help to improve the manufacturing processes.

BIBLIOGRAPHY

[1] European Commission: Emissions in the automotive sector; Available from: https://www.sciencedirect.com/topics/engineering/sheet-molding-compounds.

[2] Kirvan K, Wood B. Recycling of materials in automotive engineering from Advanced Materials in Automotive Engineering.

[3] Stelzer P. Experimental feasibility and environmental impacts of compression molded discontinuous carbon fiber composites with opportunities for circular economy.: Composites Part B: Engineering, 2022. 234. Article: 109638.

[4] SMC BMC Drive Composite Innovation.: SMC/BMC Design Guide 1; Available from: https://smcbmc-europe.org/publications_pdf/SMCBMC-A4-DESIGN-GUIDE-1.pdf.

[5] Mertiny P, Ellyin F. Composites Part A: Applied Science and Manufacturing: Influence of the filament winding tension on physical and mechanical properties of reinforced composites; Available from: https://doi.org/10.1016/S1359-835X(02)00209-9.

[6] Abdalla F, Mutasher S, Khalid Y.A, Sapuan S.M, Hamouda A, Sahari B.B et al. Design and fabrication of low cost filament winding machine; Available from: https://doi.org/10.1016/j.matdes.2005.06.015.

[7] Azeem M, Haji Ya H, Azad Alam, Mohammad, Kumar, Mukesh, Stabla, Pawet, Smolnicki M, Gemi L, Khan R et al. Application of Filament Winding Technology in Composite Pressure Vessels and Challenges; Available from: https://doi.org/10.1016/j.est.2021.103468.

[8] Früh N, Knippers J. Multi-stage filament winding: Integrative design and fabrication method for fibre-reinforced composite components of complex geometries; Available from: https://doi.org/10.1016/j.compstruct.2021.113969.

[9] Peters S. Composite Filament Winding: ASM International; 2011.

[10] The Composites Hub. Filament Winding. A cost-effective composites process; Available from: https://www.thecompositeshub-india.com/filament-winding--a-cost-effective-composites-process.

[11] Minsch N, Herrmann F, Gereke T, Nocke A, Cherif C. Analysis of filament winding processes and potential equipment technologies; Available from: https://doi.org/10.1016/j.procir.2017.03.284.

[12] Kenny JM, Nicolais L. Comprehensive Polymer Science and Suplements: Suplement 1; 1996.

[13] Donnet J-B, Wang TK, Peng JC. Carbon Fibers; 1998.

[14] Khurshid MF, Hengstermann M, Hasan MMB, Abdkader A, Cherif C. Recent developments in the processing of waste carbon fiber for thermoplastic composites: A review. Journal of Composite Materials; Available from: https://doi.org/10.1177/0021998319886043.

[15] Product Development Prototypes Parts GmbH KOHLENIA S.R.L. Deepflow. Development and processability assessment of a new recycling Sheet Molding Compound material with numerical endorsement; Available from: https://www.asg.ed.tum.de/lcc/oeffentliche-projekte/simulation/deepflow-development-and-processability-assessment-of-a-new-recycling-sheet-molding-compound-material-with-numerical-endorcement/.

[16] Lee H, Huh M, Yoon J, Lee D, Kim S, Kang S. Fabrication of carbon fibers SMC composites with vinyl ester resin and effect of carbon fiber content on mechanical properties; Available from: http://dx.doi.org/10.5714/CL.2017.22.101.

[17] Park C. Compression Molding in polymer matrix composites.

[18] Advanced Composite Materials Selector guide. Compression Molding & Bulk Molding Compounds (BMC); Available from: https://www.toraytac.com/media/c6213225-7e36-45f0-be50-e80e5b60a5ab/hhyOcQ/TAC/Documents/Selector%20Guides/Toray_CompressionMoldedParts_DINA4_broch_v4.9.pdf.

[19] Fu Y, Yao X. A review on manufacturing defects and their detection of fiber reinforced resin matrix composites; Available from: https://doi.org/10.1016/j.jcomc.2022.100276.

[20] ASTM International. Standard Test Method for Tensile Po.

[21] Davis JR. Tensile Testing; Available from: 2004.

[22] Module 8. Composite Testing: Tensile and Compressive Testing. Tensile Testing; Available from: https://archive.nptel.ac.in/content/storage2/courses/101104010/lecture37/37_5.htm.

[23] International. Standard Test METHOD FOR Tensile Properties of Polymer Composite Materials; Available from: https://cstjmateriauxcomposites.wordpress.com/wp-content/uploads/2018/04/d3039d3039m.pdf.

[24] Understanding Composite Compression Test Methods; Available from: https://www.element.com/nucleus/2020/composite-compression-test-methods.

[25] ASTM International.

[26] Composites Test Fixtures. Compression; Available from: https://www.instron.com/-/media/literature-library/products/2014/08/composite-compression-unsupported-gage-section.pdf?&ch=109&sc_lang=en&ch=280.

[27] Understanding ASTM D6641. Compressive Properties (CLC) ASTM D6641; Available from: https://www.materialtestingexpert.com/polymer/compressive-properties-clc-astm-d6641.

[28] DIN EN ISO. DIN EN ISO 14125: Deutsche norm. Bestimmung der Biegeeigenschaften; 1998.

[29] ASTM International. Flexural Test ASTM D7264; Available from: https://www.addcomposites.com/post/mechanical-testing-of-composites#viewer-esuah.

[30] Hamid WWA, Ianucci L, Robinson P. Flexural behavior of 3D-printed carbon fiber composites: Experimental and virtual tests applications to composite adaptive structure; Available from: https://doi.org/10.1016/j.jcomc.2022.100344.

[31] Bahnart D, Monir S, Durieux O, Dary RJ, Jones M. A review of experimental and numerical methodologies for impact testing of composite materials; Available from: https://doi.org/10.1080/28361466.2024.2304886.

[32] AENOR. UNE EN ISO 179-1. Plastics. Determination of Charpy impact properties.: Part 1: Non-instrumented impact test; 2019.

[33] Leroux P. Composite Material Analysis using 3D Profilometry; Available from: https://www.researchgate.net/publication/340870151_Composite_Material_Analysis_using_3D_Profilometry.

[34] OLIN. SAFETY DATA SHEET. D.E.R. 383.

[35] HUNTSMAN. MATERIAL SAFETY DATA SHEET. JEFFAMINE D 230.

[36] KOHLENIA. DEEPFLOW. MATERIAL DEFINITION.

[37] Massen und Volumenanteile BMC Platten Zugproben.

[38] ASTM International. Standard Test Method for Tensile Properties of Polymer Matrix Composite Materials. https://www.astm.org/d7264_d7264m-21.html; 2014.

[39] Imbsweiler AJ, Shinoura Y, Colin D, Zaremba S, Drechsler K. Towards a Holistic Approach for an Efficient Determination of the Rheological Behavior of Sheet Molding Compounds for Process Simulation; Available from: https://www.researchgate.net/publication/362211630_Towards_a_Holistic_Approach_for_an_Efficient_Determination_of_the_Rheological_Behavior_of_Sheet_Molding_Compounds_for_Process_Simulation.

[40] Wang J. Setup of Material Cards for Flow Simulation of SMC and BMC Material Made with Recycled Wet Carbon Fibers from Winding; 2024.

LIST OF FIGURES

LIST OF TABLES

APPENDIX

A Tensile Test Specimens

For all the specimens, they are represented by three pictures. On the left, the front view is shown, followed by the side view, and finally, on the right the back view.

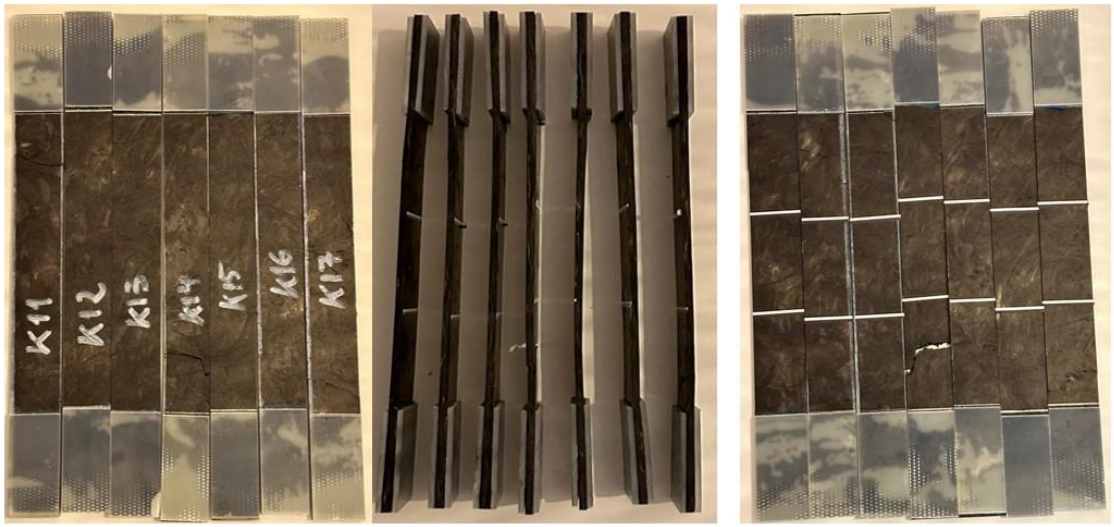

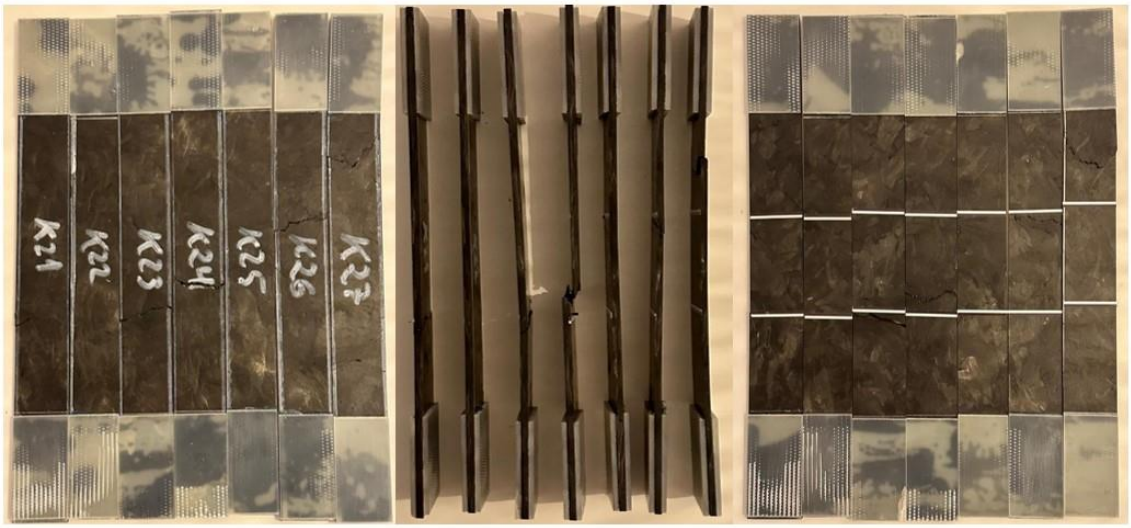

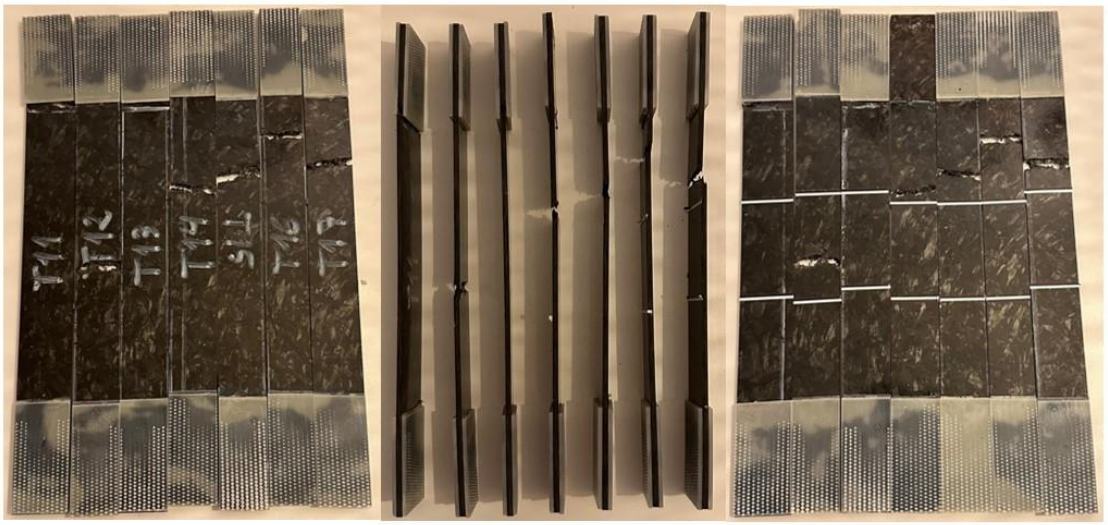
T11 T12 T13 T14 T15 T16 T17
T11 T12 T13 T14 T15 T16 T17
T11 T12 T13 T14 T15 T16 T17

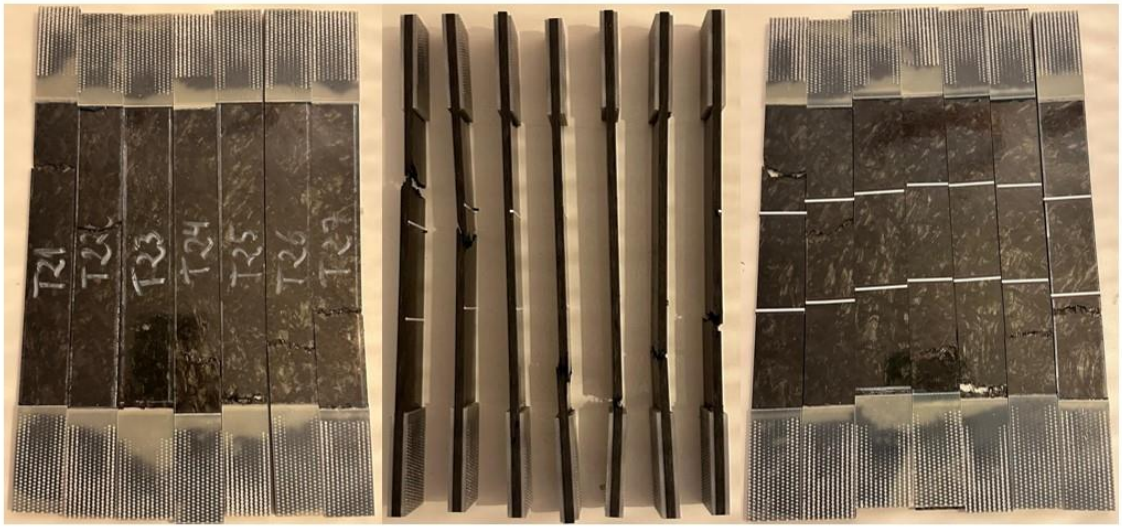
T21 T22 T23 T24 T25 T26 T27
T21 T22 T23 T24 T25 T26 T27
T21 T22 T23 T24 T25 T26 T27

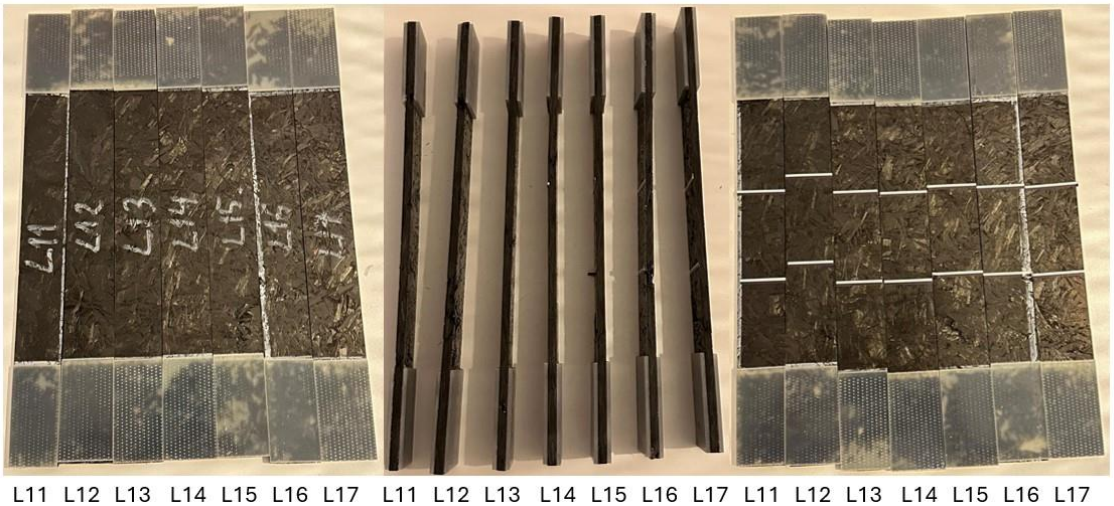
L11 L12 L13 L14 L15 L16 L17
L11 L12 L13 L14 L15 L16 L17
L11 L12 L13 L14 L15 L16 L17

B Flexural Test Specimens

For all the specimens, they are represented by three pictures. On the left, the front view is shown, followed by the side view, and finally, on the right the back view

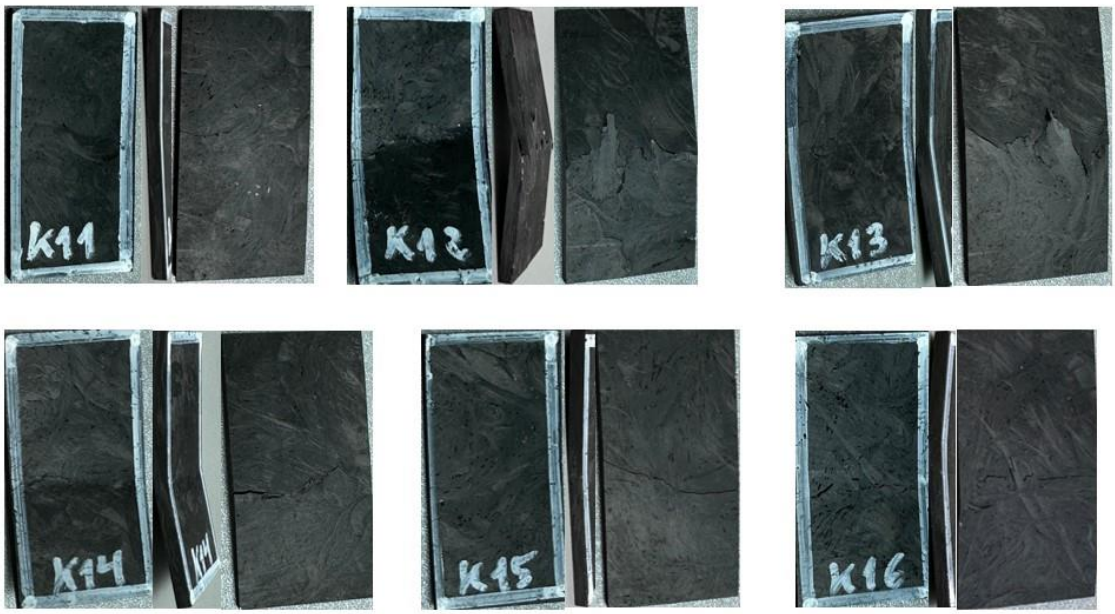

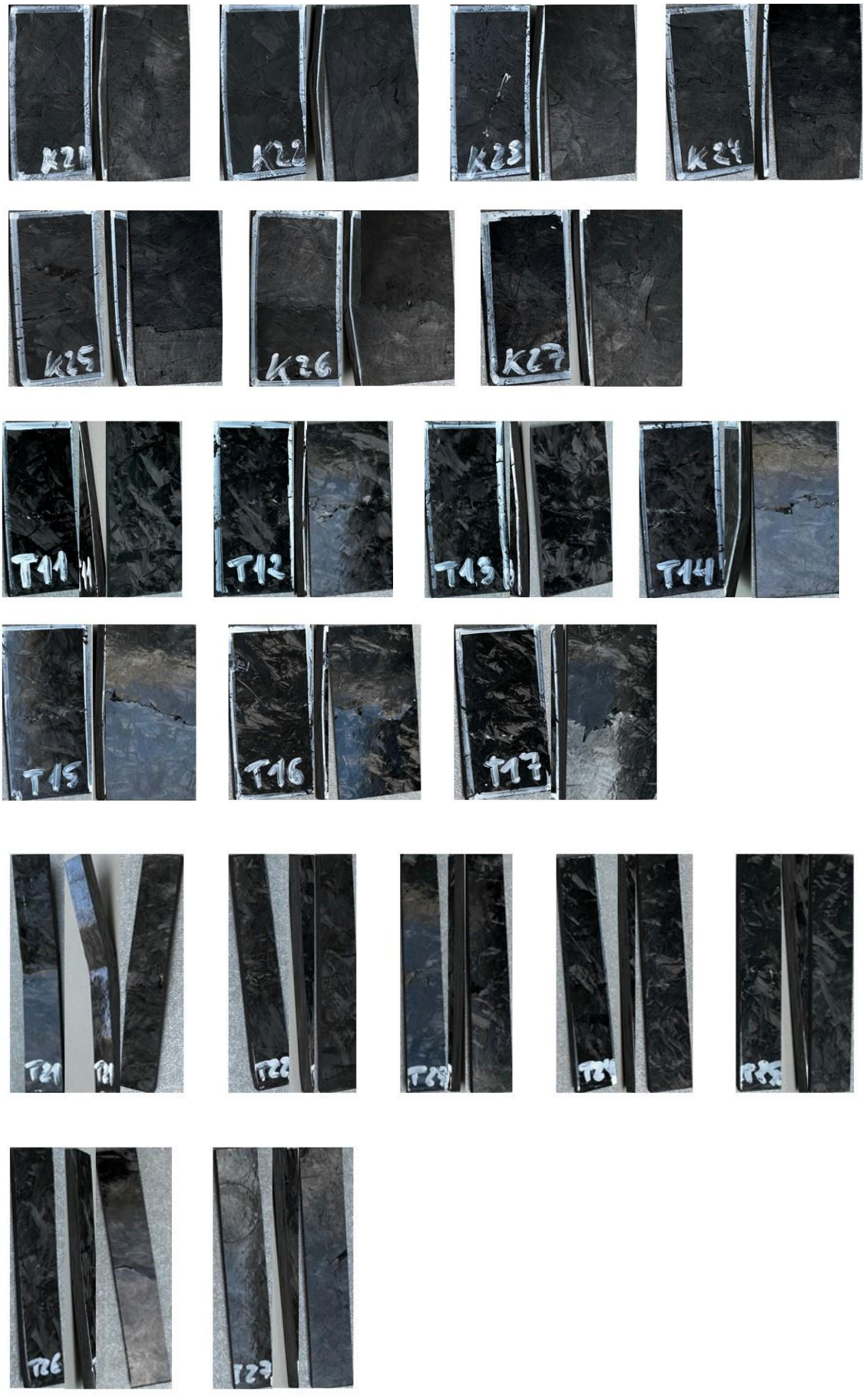
K21
K22
K23
K24
K25
K26
K27
T11
T12
T13
T14
T15
T16
T17
T21
T22
T23
T24
T25
T26
T27